

**DEVELOPMENT AND CHARACTERIZATION OF
ELECTROSPUN POLYACRYLONITRILE-BASED
NANOCOMPOSITE MEMBRANES FOR OIL-WATER
SEPARATION**

BY

NOMAN NASEEB

A Thesis Presented to the
DEANSHIP OF GRADUATE STUDIES

KING FAHD UNIVERSITY OF PETROLEUM & MINERALS

DHAHRAN, SAUDI ARABIA

In Partial Fulfillment of the
Requirements for the Degree of

MASTER OF SCIENCE

In

MATERIALS SCIENCE AND ENGINEERING

DECEMBER 2017

KING FAHD UNIVERSITY OF PETROLEUM & MINERALS

DHAHRAN- 31261, SAUDI ARABIA

DEANSHIP OF GRADUATE STUDIES

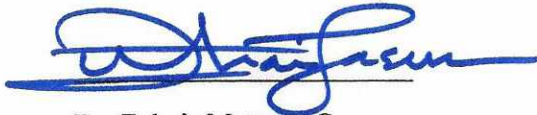
This thesis, written by **NOMAN NASEEB** under the direction his thesis advisor and approved by his thesis committee, has been presented and accepted by the Dean of Graduate Studies, in partial fulfillment of the requirements for the degree of **MASTER OF SCIENCE IN MATERIALS SCIENCE AND ENGINEERING**.



Dr. Tahar Laoui
(Advisor)



Dr. Zafarullah Khan
(Member)



Dr. Zuhair Mattoug Gasem
Department Chairman



Dr. Salam A. Zummo
Dean of Graduate Studies



Dr. Wail Sulaiman Falath
(Member)

4/3/18

Date

© Noman Naseeb

2017

I dedicate this thesis to my family

ACKNOWLEDGMENTS

I would like to express my heartfelt thanks to my advisor, Prof. Tahar Laoui, for his continuous support, guidance and care for my thesis. Special thanks goes to Prof. Zafarullah Khan for his in-depth knowledge about the topic and support towards the completion of this work. I would also like to thank my committee member Dr. Wail Sulaiman Falath for his help and quick responses.

Here, it is also mandatory to say thanks to Engr. Abdul Azeem for his exceptional support and guidance towards the completion of this study. Sincere appreciation should also be given to my research group members Omar, Bassel and Ahmed for making this journey towards MSc memorable. The lab engineers from materials science lab, environmental lab from civil engineering, analytical lab from chemical and chemistry departments and materials characterization lab from research institute should also be acknowledged.

I would also like to acknowledge KFUPM and DSR for giving me the scholarship and financial support. Thanks to CENT and Dr. Abbas for providing me hands-on experience of hi-tech characterization tools.

Many thanks to my family for their endless support, prayers and encouragements. Without their continuous support, it was impossible to achieve this goal.

Noman Naseeb

TABLE OF CONTENT

ACKNOWLEDGMENTS	v
TABLE OF CONTENT	vi
LIST OF TABLES	ix
LIST OF FIGURES	x
LIST OF ABBREVIATIONS.....	xii
ABSTRACT.....	xv
ملخص الرسالة	xvii
CHAPTER 1 INTRODUCTION	1
1.1 Background	1
1.2 Research objectives	3
1.3 Thesis overview.....	3
CHAPTER 2 LITERATURE REVIEW	5
2.1 Membrane-based separation.....	5
2.2 Origin of superwetting	6
2.3 Theories behind superwetting	8
2.4 Techniques for membrane fabrication.....	9
2.5 Electrospinning.....	11
2.5.1 Effect of solution concentration.....	13
2.5.2 Effect of molecular mass of polymer.....	14
2.5.3 Effect of solution conductivity.....	14
2.5.4 Effect of applied voltage.....	14
2.5.5 Effect of solution feed rate.....	15
2.5.6 Effect of spinnret to collector distance	15
2.6 Electrospun membranes in treating oily waters	15
2.6.1 Electrospun oil wetting membranes.....	15
2.6.2 Electrospun water wetting membranes	20
2.6.3 Pore size control in electrospun membranes.....	25
2.7 Proposed work based on the recent studies	25
CHAPTER 3 EXPERIMENTAL WORK	27

3.1	Materials.....	27
3.2	Fabrication of electrospun membranes	27
3.2.1	Electrospinning of PAN membrane	29
3.2.2	Electrospinning of PAN-Composite membranes.....	30
3.3	Hot pressing of electrospun membranes	32
3.4	Exposure to solvent vapors	32
3.5	Hydrolyzation of PAN-based membranes.....	32
3.6	Direct coating of GO-hydrogel	33
3.7	Characterization of electrospun membranes	33
3.7.1	Morphological examination.....	33
3.7.2	Fourier transform infrared spectroscopy.....	34
3.7.3	Wetting behavior.....	34
3.7.4	Pore size measurement.....	35
3.7.5	Membranes porosity.....	35
3.7.6	Tensile testing	36
3.8	Separation of oil and water emulsion.....	36
CHAPTER 4 RESULTS AND DISCUSSION.....		37
4.1	Parametric study.....	37
4.1.1	Effect of voltage.....	37
4.1.2	Effect of flow rate	38
4.1.3	Effect of spinneret speed.....	40
4.1.4	Effect of polymer concentration	42
4.1.5	Effect of rotational speed	44
4.1.6	Effect of needle size.....	46
4.2	Hydrolyzation of PAN-based membrane	48
4.3	Direct coating of GO-hydrogel	55
4.4	Direct exposure to solvent vapors	58
4.5	Characterization of PAN/PAN-based nanocomposite membranes.....	61
4.6	Separation testing of PAN/PAN-based nanocomposite membranes.....	75
4.7	Comparative analysis	79
CHAPTER 5 CONCLUSIONS AND RECOMMENDATIONS.....		81

5.1	Conclusions	81
5.2	Recommendations	83
	References.....	85
	Vitae.....	95

LIST OF TABLES

Table 1. Summary of approaches for oil-water separation membranes.....	9
Table 2. Recent work on oil-water separation membranes.....	26
Table 3. Composition of Pure PAN-based membranes	30
Table 4. Electrospinning dope composition of composite-hybrid membranes.....	31
Table 5. Effect of hydrolyzation on the pore size.....	51
Table 6. Surface characteristics of PAN/PAN-based membrane.....	69
Table 7. Mechanical properties of PAN/PAN-based membranes	72
Table 8. Rejection (%) and flux of PAN-based membranes after oil-water separation ...	78
Table 9. Comparison of developed hybrid electrospun membrane with similar work.....	80

LIST OF FIGURES

Figure 1. Shark fish an example of underwater superoleophobicity (a), Lotus leaf an example of superhydrophobicity (b) [15], [20].....	7
Figure 2. An illustration of Wenzel (left) and Cassie-Baxter (right) state [82]	8
Figure 3. An illustration of Electrospinning setup.....	12
Figure 4. Formation of beaded to uniform fibers is shown from (a) to (d) with an increase in solution concentration [59]	13
Figure 5. Effect of SiO ₂ loading. With increase in SiO ₂ content, thermal stability increases (a), flexibility increases (b), while Young's modulus (c) and toughness (d) decreases [75].....	17
Figure 6. SEM images showing smooth fibers of PAN (a,b), roughened PAN/APAN fibers (c,d), PAN/APAN/GO fibers (e,f) [87].....	22
Figure 7. Spindle knotted PAN/GO membrane, a) SEM image, b) TEM image, c) mechanism of demulsification of oil in water emulsion.....	23
Figure 8. Electrospinning setup, Nanon 01A.....	28
Figure 9. A schematic of electrospinning of PAN based membrane.....	29
Figure 10. Effect of voltage on PAN fiber: a-d, a & b) 18kV, c & d) 20kV, Effect of flowrate on PAN fiber e-h, e & f) 0.8ml/h, g & h) 1ml/h.....	39
Figure 11. Effect of spinneret speed on PAN fiber, a & d) 50mm/s, b & e) 70mm/s, c & f) 100mm/s.....	41
Figure 12. Effect of concentration on PAN fiber, a & b) 7wt% PAN, c & d) 8wt% PAN, e & f) 10wt% PAN, g & h) 12wt% PAN.....	43
Figure 13. Effect of collector rotational speed on PAN fiber, a & b) 0 rpm, c & d) 300 rpm, e & f) 500 rpm, g & h) 1000 rpm	45
Figure 14. Effect of needle diameter on PAN fiber, a & c) 18G (0.8mm), b & d) 21G (0.6mm).....	47
Figure 15. SEM images of hydrolyzed PAN based membranes (a), FTIR spectra of hydrolyzed PAN based membranes (b)	50
Figure 16. Wetting characteristics of hydrolyzed PAN membranes.....	52
Figure 17. Separation performance of hydrolyzed PAN based membranes, (a) permeate fluxes, (b) separation permeate images.....	54
Figure 18. FESEM images of PVA-GO coated PAN.....	56
Figure 19. Separation behavior of PVA-GO coated electrospun PAN membrane.....	57
Figure 20. Effect of exposure to DMF vapors on electrospun PAN membrane, (a-d) FESEM images of :(a) 0 min exposure, (b) 0.5min exposure, (c) 3min exposure, (d) 0.5 min exposure on hydrolyzed membrane, (e) Pore size vs time of exposure, (f) separation performance for PAN and hydrolyzed PAN membrane	60

Figure 21.(left) SEM images of PAN based membranes, a) PAN, b) PAN-4SiO ₂ , c) PAN-7.5SiO ₂ , d) PAN-11SiO ₂ , e) PAN-0.5GO, f) PAN-1.5GO, g) PAN-4GO, h) PAN-1.5GO-7.5SiO ₂ , (right) Digital images of the electrospun membranes	62
Figure 22. SEM images of SiO ₂ nano powder (a-b), TEM images of electrospun pristine PAN and PAN-1.5GO-7.5SiO ₂ membrane (c-d)	65
Figure 23. FTIR spectra (a) and XRD pattern(b) of PAN-composite electrospun membranes	67
Figure 24. Showing pore size of electrospun PAN/PAN based membranes	70
Figure 25. Water and underwater oil contact angles of PAN-composite membranes, (a)PAN, (b)PAN-1.5GO, (c)PAN-7.5SiO ₂ , (d)PAN-7.5SiO ₂ -1.5GO	74
Figure 26.Separation performance of PAN-nano composite/hybrid electrospun membranes	76
Figure 27. Separation Flux of (a) PAN-Nanocomposite, and (b) hybrid membrane	77

LIST OF ABBREVIATIONS

APAN	Aminated polyacrylonitrile
BA	Butyl Acrylate
CaCO₃	Calcium carbonate
CS	Chitosan
Cu	Copper
CNT	Carbon nanotube
F-CNT	Fluorinated carbon nanotube
CF	Carbon fabric
DA	Dopamine
GA	Glutaraldehyde
GO	Graphene oxide
MnO₂	Manganese dioxide
MWCNT	Multiwalled carbon nanotube
NW	Nanowire
NaOH	Sodium hydroxide
NF	Nanofibers

NIPAM	Poly isopropylacrylamide
OCA	Oil contact angle
PAN	Polyacrylonitrile
PANI	Polyaniline
PVDF	Polyvinylidene fluoride
PAA	Polyacrylic acid
PAA-g-PVDF	Polyacrylic acid grafted polyvinylidene fluoride
PP	Polypropylene
PU	Polyurethane
PA	Polyamide
PVDF-HFP	Poly (vinylidene fluoride-co-hexafluoropropylene)
PSF	Polysulfone
PS	Polystyrene
PEO	Polyethylene oxide
PAN	Polyacrylonitrile
PEG	Polyethylene glycol
PIM	Polymer of intrinsic micro porosity

POSS	Polyhedral oligomeric silsesquioxane
PCTE	Polycarbonate track etched
PUA	Polyurethane acrylate
PEI	Polyethyleneimine
PEPA	Polyethylene polyamine
PLA	Polylactide
SiO₂	Silica
SNP	Silica nanoparticles
SSM	Stainless steel mesh
SEM	Scanning Electron Microscope
St	Polystyrene
TiO₂	Titania
TPU	Thermoplastic poly urethane
x-PEGDA	Crosslinked Polyethylene glycol diacrylate

ABSTRACT

Full Name : Noman Naseeb
Thesis Title : Development and Characterization of Electrospun Polyacrylonitrile-based Nanocomposite Membranes for Oil-Water Separation
Major Field : Materials Science and Engineering
Date of Degree : December 2017

Oil in water emulsion is encountered in many industries including pharmaceutical, food, agriculture, textile, petroleum and metal cutting. When this emulsion goes directly to sewage, it creates environmental problems and causes wastage of enormous amounts of valuable resources. Therefore, it is crucial to develop efficient and economical techniques that can address these problems. Membrane based separation is a promising technique for efficient and cost-effective separation of oil-water emulsion. Electrospinning process for membrane fabrication provides additional advantages such as nano-fibrous porous structure and unique surface characteristics. The aim of this research is to develop polyacrylonitrile (PAN) based membranes for oil in water emulsion separation using electrospinning technique. Initially, the effect of various electrospinning process parameters was studied and optimized to achieve smallest fiber diameter along with defect free and hierarchical structure suitable for separation. Different concentrations of 2D-graphene oxide (GO) and silica (SiO_2) nanofillers were used to characterize the morphology, surface characteristic, mechanical strength and performance of PAN nanocomposite membranes. Scanning electron microscopy (SEM), fourier transform infrared spectroscopy (FTIR), pore size, contact angle measurement and tensile testing were utilized for characterization while membrane performance was evaluated using

gravity driven oil-water separation test. The results revealed that hybrid PAN membrane with 7.5 wt%SiO₂ and 1.5 wt%GO separated oil with a rejection of 99% while maintaining a water permeate flux of 3150 L.m⁻².h⁻¹, with a small flux reduction (2900 L.m⁻².h⁻¹) after five cycles of separation. The high separation performance is attributed to the enhanced hydrophilic-oleophobic properties of the hybrid membrane, possessing a water contact angle of 10° and underwater oil contact angle of 155°, due to its surface hierarchical structure resulting from silica and graphene oxide nano-additives.

ملخص الرسالة

الاسم الكامل: نعمان نصيب

عنوان الرسالة: تطوير وتوصيف الأغشية المستندة إلى النسيج الإلكتروني من البولي أكريلونيتريل لفصل الزيت عن الماء

التخصص: الهندسة الميكانيكية

تاريخ الدرجة العلمية: ديسمبر 2017

يوجد الزيت في مستحلب المياه و الزيت في العديد من الصناعات بما في ذلك الأدوية والمواد الغذائية والزراعة والمنسوجات والبتروول و قطع المعادن. عندما يذهب هذا المستحلب مباشرة إلى مياه الصرف الصحي، فإنه يخلق مشاكل بيئية ويسبب هدر كميات هائلة من الموارد القيمة. ولذلك، من الضروري تطوير تقنيات فعالة واقتصادية يمكن أن تعالج هذه المشاكل. الفصل القائم على الغشاء هو تقنية واعدة للفصل وفعالة من حيث التكلفة. عملية غزل كهربائي (Electrospinning) لتصنيع الغشاء يوفر مزايا إضافية مثل مسامية هيكل نانو-ليفية وخصائص سطح فريدة من نوعها. والهدف من هذا البحث هو تطوير أغشية البولي أكريلونيتريل (PAN) لفصل الزيت من المستحلب باستخدام تقنية الغزل كهربائي. في البداية، تم دراسة تأثير مختلف العوامل المؤثرة في عملية الغزل كهربائي والأمثل لتحقيق أصغر قطر الألياف جنباً إلى جنب مع بنية خالية من العيوب. تم استخدام تراكيز مختلفة من أكسيد الجرافين (GO) والسيليكا (SiO_2) المألثة النانومترية لوصف التشكل، سمة السطح، القوة الميكانيكية والأداء للأغشية بان المركب المتناهي الصغر. واستخدمت المجهر الإلكتروني المجهرى (SEM) والتحويل فورييه الطيفي بالأشعة تحت الحمراء (FTIR)، وحجم المسام، وقياس زاوية الاتصال واختبار الشد للتوصيف بينما تم تقييم أداء الغشاء باستخدام اختبار فصل المياه و الزيت عن طريق الجاذبية. كشفت النتائج أن غشاء بان الهجين مع SiO_2 و 1.5% بالوزن GO فصل الزيت عن المياه بنسبة 99% مع الحفاظ على تدفق المياه ($3150 \text{ L/m}^2\text{h}$)، مع انخفاض صغير في تدفق ($2900 \text{ L/m}^2\text{h}$) بعد خمس دورات من الانفصال. ويرجع الأداء المتميز في الفصل إلى تحسين خصائص مؤلفة مع الماء و الكاره للزيت من الغشاء الهجين، وتمتلك زاوية اتصال المياه من 10 درجة وزاوية اتصال الزيت تحت الماء من 155 درجة، ويرجع ذلك إلى هيكلها الهرمي السطحي الناتجة عن إضافة السيليكا (SiO_2) وأكسيد الجرافين (GO).

CHAPTER 1

INTRODUCTION

1.1 Background

Oil water separation has always remained an interesting and challenging problem among researchers for the last few decades. This interest lies in the fact that water/seawater, being a major resource, is wasted heavily in the form of oil spills/leakages from transportation units or oil processing in the offshores. Many other industries that include textile, petroleum, pharmaceutical, agriculture, polymer, food processing, leather, and metalworking are also responsible for generating huge amounts of emulsions in the form of oily wastewater [1]. These oily emulsions with droplet sizes in the submicron range ($<20\mu$) is often discharged into sewage or sometimes into the freshwater reservoirs creating serious environmental damage as well as wastage of valuable resources. Saudi Arabia, the world's largest oil producer, is also producing enormous amounts of oily emulsions, which needs to be treated in a way to save the environment. Several industries have employed wastewater treatment methods such as gravity separation (especially employed in upstream petroleum oil-water-gas separators or 3-phase separators), filtration, flotation, coagulation and other chemical methods [2]–[4]. These methods are incapable to provide satisfactory separations especially in cases of emulsions with reduced droplet sizes and also causes secondary pollutions [5].

Using membranes for separating oil-water emulsion is the most simple and cost-effective method. The membranes can either be hydrophobic-oleophilic, allowing oil to pass through or hydrophilic-oleophobic, capable of retaining oil from the emulsion. Recent developments in fabricating superwetting materials have shown promise in separating oil-water mixtures by designing superhydrophobic/superoleophilic or superhydrophilic/superoleophobic surfaces in conjunction with the morphology and chemistry of the membrane surface [6]. The major concern in this technology when used for emulsion treatment is related to fouling where oil droplets get plugged on the membrane surface or within the porous structure and hinder its longtime use [7]. Therefore, in this research, it is proposed to develop superwetting electrospun nano-fibrous membrane capable of separating oil from oil in water emulsions effectively and economically than the existing membrane technology. Polymeric materials and their blends with nanofillers will be utilized to develop such highly porous membranes with high specific surface areas using electrospinning technique. This technique has been considered promising for producing nanofiber mats due to the flexibility of control over fiber diameter and morphology, but also provides means of large-scale production.

Thus, the main objective of the proposed research is to develop superwetting membrane for the separation of oil and water from their emulsified mixture. Electrospinning technique is used to fabricate nanofiber polymeric mats with suitable chemistry and surface properties. Process optimization is carried out to obtain the best combination of fiber diameter, pore size, and surface morphology. The nanofiber mats are characterized and evaluated to determine the most efficient oil-water separation characteristics.

1.2 Research objectives

The aim of this research is to develop an electrospun hybrid polyacrylonitrile (PAN)-silica (SiO₂)-graphene oxide (GO) membrane which can be used for efficient and reusable separation of water and oil from the emulsified mixture. It encompasses the following objectives:

- Fabrication of pristine PAN membrane using the electrospinning process.
- Variation of the process parameters to obtain PAN membrane with the best combination of fiber diameter, pore size, porosity and surface morphology.
- Fabrication of PAN-SiO₂ and PAN-GO nanocomposite membranes.
- Fabrication of PAN-SiO₂-GO hybrid membrane.
- Characterization and evaluation of the developed mats to determine the most efficient oil-water separation characteristics.

1.3 Thesis overview

This thesis comprises five chapters:

Chapter 1 gives a brief introduction of the topic, its importance and the objectives of the present work

Chapter 2 provides literature on the latest research in this area. This chapter starts with an introduction of principles behind membrane-based separations, followed by the

methods used for membrane fabrication, an explanation of electrospinning method, related work, ending with the proposed approach for this work.

Chapter 3 outlines the methodology used in this work towards the fabrication and characterization of the electrospun membranes.

Chapter 4 presents the results and discussion of the characteristics and performance of the developed electrospun membranes.

Chapter 5 concludes the thesis along with recommendations for future work.

CHAPTER 2

LITERATURE REVIEW

2.1 Membrane-based separation

Membranes are considered as a selective barrier that allows specific constituent of a mixture to pass through while rejecting the other constituent. They are used in many applications such as gas separators [8], drug delivery [9], anti-icing [10], drag reduction [11], membrane distillation [12], and so on. It is the membrane's chemical nature and the surface properties along with the pore size that make them suitable for various applications. Among the membrane's characteristics, hydrophobicity and hydrophilicity are the key aspects defining the performance of a membrane system. These properties are collectively called super-wetting properties. New applications are constantly explored for the membrane technology. One such application is that of oil-water separation from a mixture of their emulsion.

At this point, it is important to define the types of oil-water mixtures which could fall into three categories: Free oil, where oil droplet size is $> 150 \mu\text{m}$, dispersed oil, where oil droplet size is between $20\text{-}150 \mu\text{m}$ and emulsified oil, where oil droplet size is $< 20 \mu\text{m}$. thus, an emulsion that contains micro-nano sized oil droplets is the most difficult to treat through conventional routes and highly efficient membrane system is required.

It is vital for the separation of oil from a mixture of oil and water that the membrane surface should have characteristics of superhydrophobicity/oleophilicity or

superhydrophilicity/oleophobicity, thus water or oil can pass through while rejecting the other. In addition to the surface chemistry, the membrane should also have a pore size smaller or comparable to the emulsion droplet size.

2.2 Origin of superwetting

The idea behind superwetting surfaces comes up from nature creatures such as lotus leaf. In early 90's, it was discovered by a team of scientists headed by Barthlott [13] that the lotus leaves (figure 1) with epicuticular wax type structures don't require pre-cleaning stage for SEM examination while others with smooth surface structures require cleaning. It was surface's superhydrophobic nature that renders the surface with self-cleaning ability. The idea of superoleophobicity comes from the shark and some other fish (figure 1), the skin of these species repel oil and does not allow it to accumulate while being wetted by sea water [14]. This unique property is believed to be due to the hydrophilic surface mucus and multiscale surface structures composed of the sector like scales with diameters in millimeters covered by papillae with dimensions in micrometers. A surface that shows hydrophilicity and oleophilicity in the air, can be oleophobic when pre-wetted with water [15].

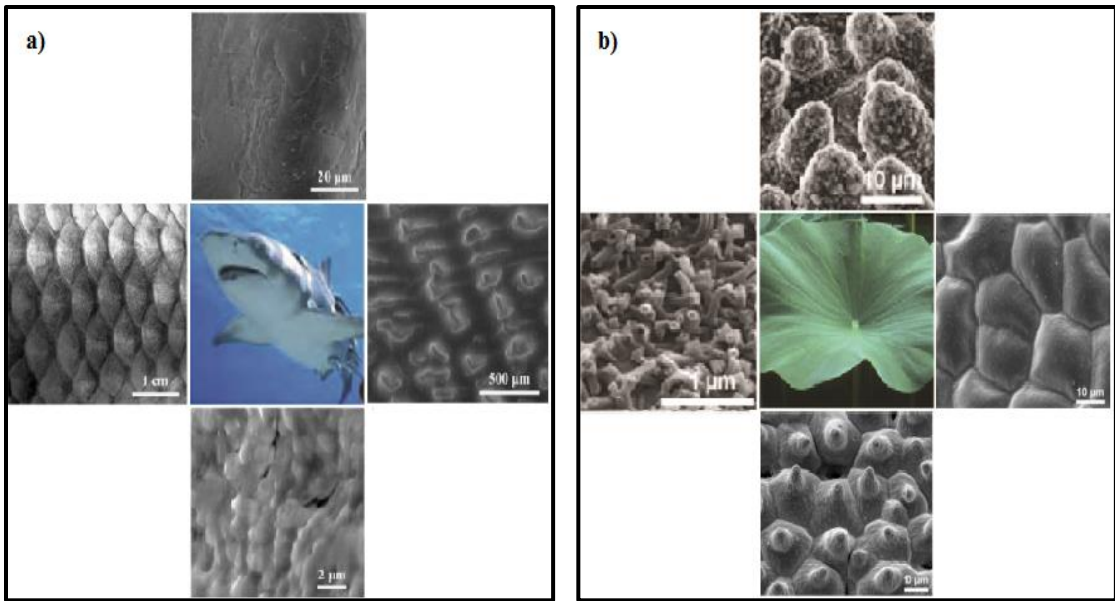


Figure 1. Shark fish an example of underwater superoleophobicity (a), Lotus leaf an example of superhydrophobicity (b) [15], [20]

2.3 Theories behind superwetting

It is important to mention here that Wenzel and Cassie-Baxter set forth two theories that form the backbone of superwetting. In the Wenzel state, the liquid droplet fully wets the surface with textures [16] while in Cassie-Baxter state, the liquid drop is supported by the surface composed of solid and the air-trapped in between makes the surface hydrophobic (figure 2). Air is the most hydrophobic and oleophobic with intrinsic contact angles of > 180 . So, materials with hydrophilic or oleophilic nature in the smooth surface may be transferred to hydrophobic or oleophobic comprising rough surfaces in the Cassie-Baxter state. Thermodynamically for low surface tension liquids such as oil, Cassie-Baxter state is not a stable state. That is why superhydrophobicity is more favorable compared to superoleophobicity [17], [18]. To get superoleophobicity, a re-entrant surface texture (trapezoid, spherical or cylindrical texture) is required to ensure the metastable Cassie-Baxter state whose transition to stable Wenzel state requires the system to cross an energy barrier of second Cassie-Baxter state. Thus by providing an energy barrier could lock the system in the Cassie-Baxter state of smaller free energy [19].

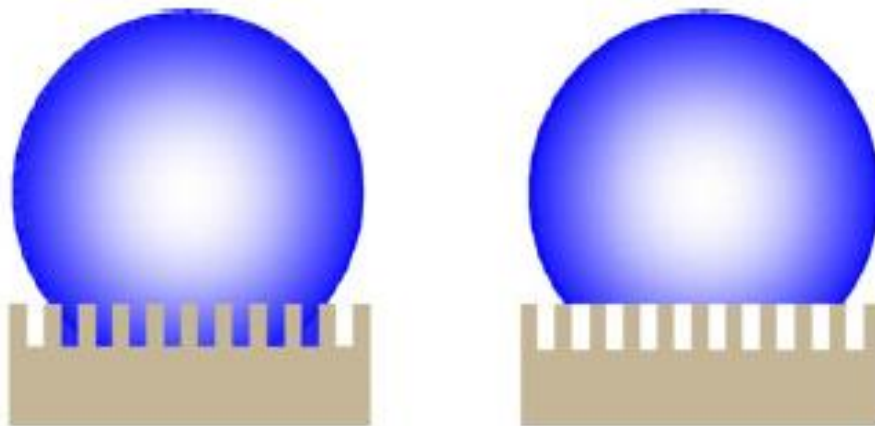


Figure 2. An illustration of Wenzel (left) and Cassie-Baxter (right) state [82]

2.4 Techniques for membrane fabrication

Porous membranes mats are produced in several ways to cater the needs of ever-increasing demand for separating an oil and water emulsion. Some of the commonly used methods to fabricate membranes are phase inversion [20]–[30], layer by layer deposition [31]–[34], dip coating [35]–[38], sol-gel [39], vacuum filtration [40], [41] and electrospinning. Some approaches are summarized in table 1.

Table 1. Summary of approaches for oil-water separation membranes

Materials	Method	Wetting behavior	Flux L.m⁻².h⁻¹	Ref
F-CNTs on CF	Chemical wet fluorination + spin coating	Superhydrophobic	1800	[42]
PANI on SSM/PVDF	coating (one step dilute polymerization)	Superoleophobic	3238	[35]
CaCO ₃ /PAA grafted PP	Grafting + alternate soaking	superoleophobic	2000	[43]
PA on NaOH/PSF	Electrospinning + interfacial polymerization	Superoleophobic	229	[44]
Cellulose on PVDF-HFP	Electrospinning + direct coating	Superoleophobic	1780	[45]
x-PEGDA)/PEO on PAN/PEG	Electrospinning + crosslinking	Oleophobic	5000	[46]

Materials	Method	Wetting behavior	Flux L.m⁻².h⁻¹	Ref
SiO ₂ /Carbon	Electrospinning + interfacial polymerization + carbonization	hydrophobic	100	[47]
PIM-1/POSS	Electrospinning	Superhydrophobic	1097	[48]
PAA-g-PVDF	Salt-induced phase inversion	superoleophobic	120	[22]
MnO ₂ NW	Suction filtration	superoleophobic	-	[49]
PVDF	In situ elimination	superhydrophobic	189	[50]
CS-SiO ₂ -GA on PVDF	Coating	superoleophobic	-	[51]
DA/TiO ₂ decorated PVDF	one step Dip coating (mussel inspired)	Superoleophobic	605	[52]
PANI/TiO ₂ NF in PVDF	Phase inversion + water coagulation	Oleophobic	132	[53]
PU on Cu mesh	Electrospinning	Hydrophobic	2483	[54]
PUA-SNP /PEI on PCTE	Layer by layer coating (dipping)	Oleophobic	-	[55]

Materials	Method	Wetting behavior	Flux L.m⁻².h⁻¹	Ref
PVDF	Phase inversion	Superhydrophobic	850	[21]
BA/St	Electrospinning	Superhydrophobic	-	[56]
NIPAM on TPU	Force spinning + dip coating	Superoleophobic	-	[57]

2.5 Electrospinning

Electrospinning is perhaps the most versatile process for fabricating nano-fibrous membranes. Nanofibers are defined as fibers with diameters in the order of 100 nanometers. As one-dimensional nanomaterials, nanofibers have an extremely high specific surface area to volume ratio and they are highly porous with excellent pore connectivity. These unique characteristics together with functionalities from fiber materials provide nanofibers with many outstanding properties as separation/filtration membranes [58]. Variety of polymers can be electrospun with different fiber morphology and properties showing the potential application in different fields from drug delivery to fuel cells [54], [59]–[66]. Electrospinning uses an electric field to charge a jet of polymeric solution. As the jet travels in the air, the solvent in the solution evaporates leaving behind the charged fiber, which is collected on a metal collector (figure 3). However, what makes electrospinning different from other nanofiber fabrication processes is its ability to obtain long length fibers with various morphologies from very rough to smooth. The desired fiber

morphology can be obtained by controlling the solution and process parameters in electrospinning [67]. In addition, different fiber sizes, diameter distribution, membrane thickness and pore size can be controlled in order to optimize the filtration by selectively rejecting the desired size particles [68]. In the next section, some of the processing parameters and their effect on the final morphology is discussed.

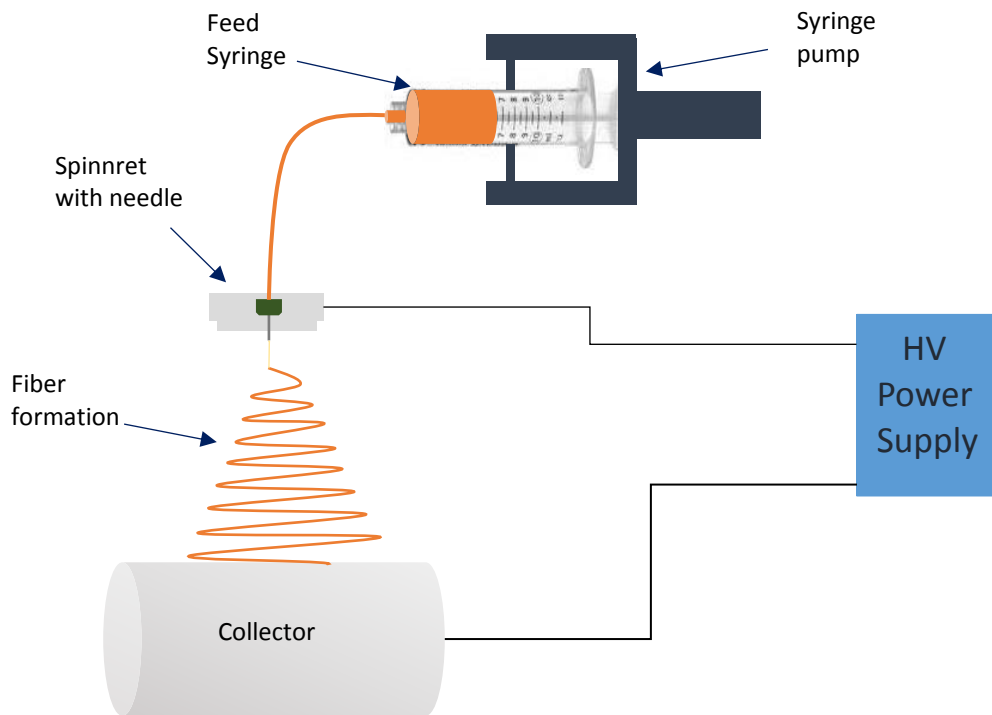


Figure 3. An illustration of Electrospinning setup

2.5.1 Effect of solution concentration

Solution concentration is by far the most important parameter to control the final fiber morphology. Increasing the solution concentration results in thickening of fibers while a decrease below a threshold value causes in dripping or electrospaying instead of electrospinning. Beaded to smooth fibers and smooth fibers (figure 4) to instability of electrospinning can be observed from very low to very high solution concentration [59], [69].

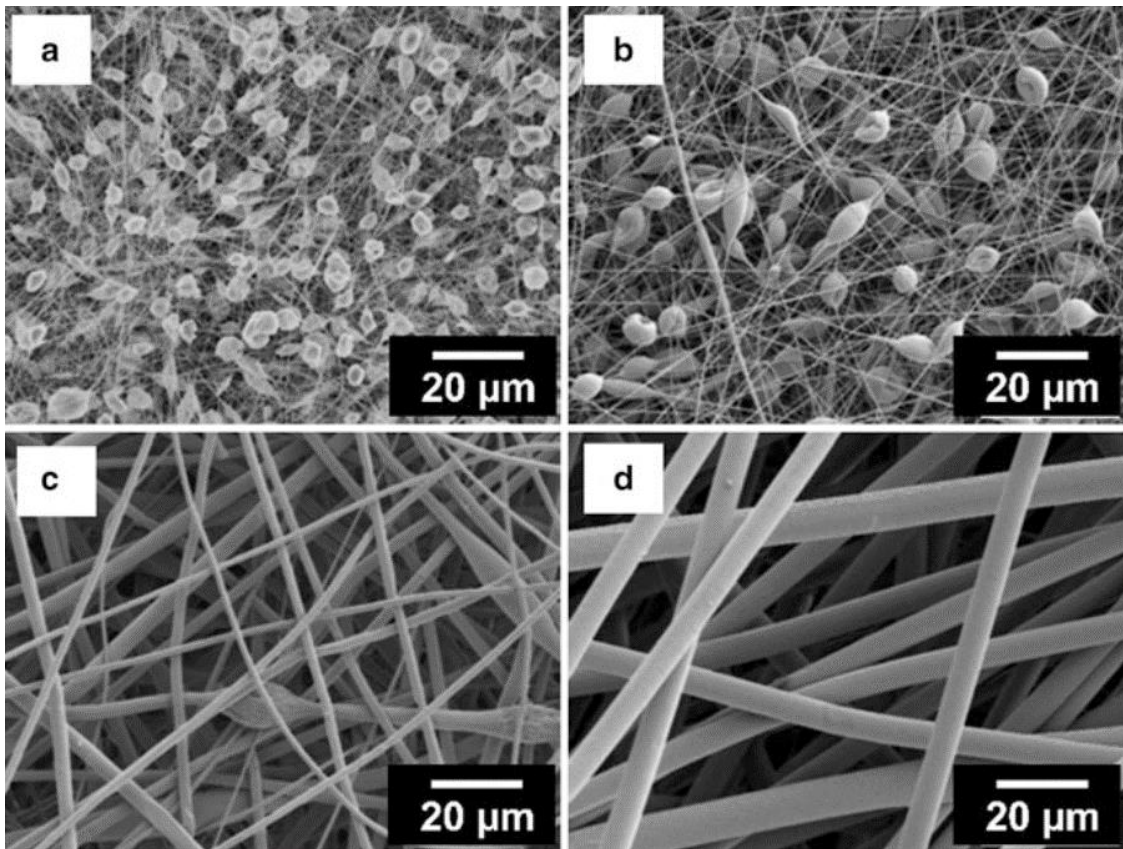


Figure 4. Formation of beaded to uniform fibers is shown from (a) to (d) with an increase in solution concentration [59]

2.5.2 Effect of molecular mass of polymer

Molecular mass has the similar effect as that of the concentration of polymer. Keeping the concentration fixed, a decrease in molecular mass causes a decrease in fiber diameter and formation of the beaded structure is observed due to the decline in solution viscosity [70].

2.5.3 Effect of solution conductivity

For electrospinning to be established, a polymer solution should have enough charges (repulsive forces) to overcome the surface tension forces. Thus, stretching of solution jet is dependent on the charge carrying ability (conductivity) of the polymer solution. Higher conductivity results in more repulsive forces, causes fibers to shrink in smaller diameters. Insufficient solution conductivity results in lower stretching of the jet hinder the formation of uniform fibers [71], [72].

2.5.4 Effect of applied voltage

Sufficient voltage is an important element in the generation of fibers, as it can overcome the surface tension and causes generation of stable Taylor cone and fiber jet. Increase in voltage also results in narrowing of fiber diameter [73]. But the effect of voltage on fiber diameter is not straightforward and there are reported literature which says that an increase in voltage causes the broadening of fiber diameter [74]. Thus it can be said that the influence of voltage is mainly dependent on the solution properties[75].

2.5.5 Effect of solution feed rate

Solution feed rate has also the major influence on the resultant fiber diameter and morphology. A low feed rate, will cause a high evaporation during jet travel towards collector, results in thinner fibers while a high flow rate will not allow sufficient solvent evaporation, thus thicker fibers with beads will be obtained [76].

2.5.6 Effect of spinnret to collector distance

The distance between the spinnret and the grounded collector is another important parameter in electrospinning. An optimum distance is required for the fibers to have enough time for solvent evaporation while a too high or too low distance will cause the formation of beads and merging of fibers at the junction points due to the presence of unevaporated solvent [77], [78].

2.6 Electrospun membranes in treating oily waters

Recently electrospun nanofiber membranes have proven to be effective medium in separating oil-water mixtures and emulsions [79], [80]. Both oil wetting and water wetting membranes through electrospinning have been fabricated and will be highlighted in the next two sections.

2.6.1 Electrospun oil wetting membranes

Oil wetting membranes are designed to reject water while allowing oil to permeate. They are superhydrophobic and superoleophilic both in air and water based on surface energies.

Many researchers have worked to develop such membranes by the process of electrospinning and are discussed below.

Lee et al. [81] prepared superhydrophobic-superoleophilic membrane by depositing polystyrene (PS) nanofibers onto a stainless steel mesh using electrospinning technique. The contact angles of diesel oil and water on the prepared PS nanofiber membrane were 0° and $155^\circ \pm 3^\circ$ respectively. The solution for electrospinning was prepared by dissolving PS ($M_w = 192,00 \text{ kg/kmol}$) in Dimethylformamide. Electrospinning was carried out at a voltage of 5 kV with a flow rate of 180 $\mu\text{L/h}$ in a needle size of 0.25mm inner diameter. The beads in the membrane were prevented by adding a small amount of nitric acid in PS solution which increased maximized electrical conductivity and minimized the effect of surface tension. This helped in a uniform fiber distribution with an average fiber diameter of 317nm. The performance of the membrane was found to be efficient in both gravity driven and pressure-driven separation tests.

Tai et al. [82] proposed a novel free-standing and flexible carbon–silica composite nanofibrous membrane fabricated by electrospinning followed by thermal treatment for oil-water separation. The mechanical strength of as-prepared membrane was found to be sensitive to SiO_2 concentration with an optimized value of 2.7 wt. % (Figure 5). The Carbon silica composite for electrospinning was prepared by mixing polyacrylonitrile ($MW = 150,000 \text{ g/mol}$, 7 wt. %) and tetraethylorthosilicate (0.5–5 wt. %) both acting as a precursor for carbon nanofiber and SiO_2 respectively. Dimethylformamide and acetic acid (volume ratio of 15/1) was used as a solvent for preparing the spin dope. The electrospinning was carried out at approximately 0.6–0.8 kV/cm with solution feeding rate of 9–10 $\mu\text{L/min}$ using a rotating drum collector. The electrospun composite membrane showed ultra-hydrophobic

and superoleophilic properties with water (WCA) and oil contact angles (OCA) of $144.2 \pm 1.2^\circ$ and 0° , respectively. The characterization results also indicated that SiO_2 was responsible for good thermal resistance for the membrane. The composite membrane was tested by a cross-flow microfiltration experiment. The effect of operating parameters on the separation performance was investigated to find the optimum conditions. It was found that increasing the pressure, increases flux initially, while a decreasing trend was observed as the pressure increases more due to droplets accumulation, finally after permeation of accumulated droplets with increased pressure, the flux again increases. Thus, the optimum pressure of 0.07 - 0.206 bar with a high cross-flow velocity was realized. Oil permeation flux of greater than $100 \text{ L}\cdot\text{m}^{-2}\cdot\text{h}^{-1}$ was reported during the separation of oil-water emulsions.

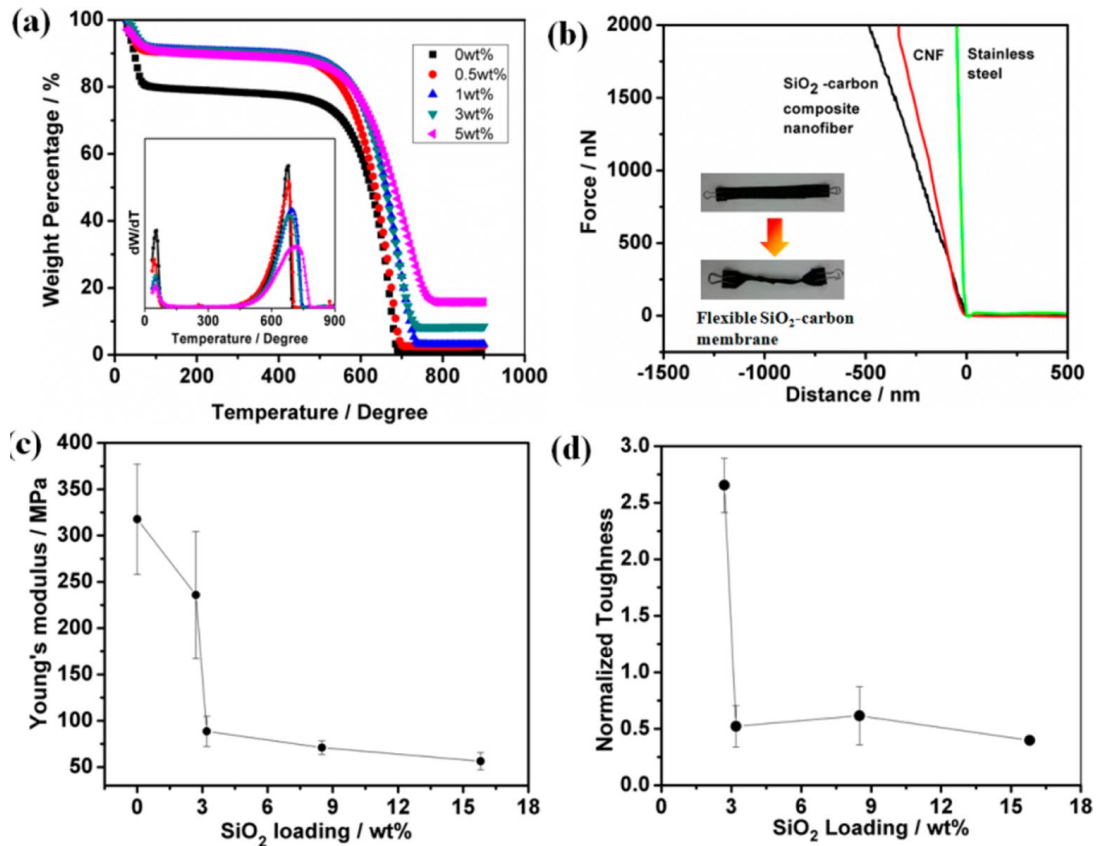


Figure 5. Effect of SiO_2 loading. With increase in SiO_2 content, thermal stability increases (a), flexibility increases (b), while Young's modulus (c) and toughness (d) decreases [75]

Researchers were also able to electrospun composite mixtures of polymeric solution for developing membranes [83]. A hybrid membrane consisting of poly (vinylidene fluoride-co-hexafluoropropylene) and fluorinated polyhedral oligomeric was developed that exhibited differential wetting (highly hydrophobic/superoleophilic) behavior for water and oil. The nanofiber membrane could efficiently separate low viscous oil from water in a single step with a separation efficiency of more than 99.99%. Furthermore, the results demonstrated that the membranes were robust and durable exhibiting differential wettability even after several oil-water separation cycles.

In another study, styrene mixed with butyl acrylate in DMF solvent was electrospun to synthesized oil-water separation membrane. Both polymers were oleophilic, but the membranes produced with the only polystyrene shows poor low-temperature flexibility and low strength. Therefore, butyl acrylate was added to improve strength. It was observed that as the content of BA increases the membrane surface becomes less hydrophobic due to a reduction in surface roughness, although at maximum concentration, the membrane still behaves hydrophobic (WCA: 155) and separates oil-water emulsion. The maximum oil separation efficiency obtained was 97.3%, which was found directly proportional to the oil content in emulsion [84].

Fang et al. fabricated membranes with the distinctive property of self-healing via electrospinning method. Membranes with surface micro/nanoscale roughness were developed using polyurethane combined with fluorine compound (PU-C8F17), which serves as self-healer, goes to the surface to maintain superhydrophobic characteristics if any surface damage occurs. It could separate both free oil-water mixtures and emulsified

mixtures with efficiency greater than 99%. The membrane allows oil to permeate with the minimum flux of $2500 \text{ L.m}^{-2}.\text{h}^{-1}$ while retaining water [54].

Ma et al. [85] fabricated membranes with asymmetric three-layered non-woven fibers consisting of different fiber diameters (in the range of 5 nm to 20 μm). An ultra-fine cellulose nano-fiber layer was used as the barrier layer. These membranes were reported to have 2-10 times increase in permeation flux over commercial membranes for ultrafiltration of oil and water emulsions.

Smart materials with interchangeable wetting characteristics are the new candidates in the field of filtration media. Studies are now going on to develop membranes that can change their behavior under different operating conditions. Che et al. [86] have produced highly porous and carbon dioxide (CO_2) switchable membrane using copolymers of PMMA (polymethylmethacrylate) and PDEAEMA (poly N, N-diethylaminoethyl methacrylate) by electrospinning. PMMA addition improves water stability of the polymer. For comparative purposes, the spinning of the same solution was also established and found that the water contact angle for the latter was about 90° while for the former, WCA was 140° . The reason for this difference in contact angle was suggested to be due to the increase in surface roughness resulted from electrospinning. To evaluate the switching property of the electrospun membrane, CO_2 purging was performed which resulted in wettability transition from hydrophobic to oleophobic. This wettability transformation could be due to the swollen and mobilization of PDEAEMA chains in the presence of water and CO_2 , making water to be captured. Exposing membrane to nitrogen could transform the membrane back to the hydrophobic state. Atomic force microscopy revealed that the CO_2 exposure made the membrane rougher, which could be a reason for changing wettability.

2.6.2 Electrospun water wetting membranes

The field of membrane technology for treating oily waters is experiencing challenges over the development of membranes that are fouling resistant to oil droplets which could be considered as a major organic foulant. To solve the issue of membrane fouling, development of highly water wetting membranes could be an option. These membranes are superhydrophilic and superoleophilic membranes in the air while superoleophobic under water. The reason for different oil wettability in air and water comes from the surface energy considerations. Thus, getting these types of membranes are difficult and requires sophisticated process optimizations.

Zhang et al. have studied the effect of graphene oxide (GO) on the performance of polyacrylonitrile membrane in oil-water separation [87]. Firstly, polyacrylonitrile (PAN) membrane was electrospun and then treated with diethylenetriamine (DETA) to enhance surface roughness. Finally, GO modification was conducted through acylation and nucleophilic reactions by immersing the DETA treated electrospun PAN membrane into graphene oxide solution thus GO/PAN membrane was obtained.

SEM examination (figure 6) revealed that compared to smooth fibers of PAN membrane, the modified graphene oxide (GO)/aminated polyacrylonitrile (APAN) membrane composed of a hierarchical structure in such a manner that the GO sheets, which are comparatively smaller, covered the PAN fibers, while larger sheets have crosslinked the PAN fibers, thus reinforcing the fibers. In oil-water emulsion separation test, the separation efficiency of greater than 99% was observed when continuous water phase quickly permeates (flux of $10000 \text{ L.m}^{-2}.\text{h}^{-1}$) through the modified membrane while emulsified oil

retained and blocked by the membrane. The unmodified membrane also showed the same permeation flux, but the discharge contains some oil and cannot meet the efficiency targets. Surface treated electrospun membranes has also been studied for treating oil-contaminated waters. Hydrolyzation through immersion in sodium hydroxide solution could be beneficial to improve membrane's hydrophilicity by converting the nitrile group in polyacrylonitrile (PAN) based membranes to more hydrophilic carboxylic acid group. The same group has also developed hydrolyzed PAN-based electrospun membranes with added benefits from antifouling graphene oxide (GO). Formation of spindle knot structure due to GO, causes the dispersed oil droplets to reunite in bigger droplets, thus goes out and demulsified (figure 7). They have reported a high permeate flux of $3500 \text{ L.m}^{-2}.\text{h}^{-1}$ with a rejection efficiency of 99% for hydrolyzed membranes containing 7% GO in PAN-based membranes [88]. Fadali et al. were able to develop composite membrane using polysulfone nanofibers synthesized using electrospinning [44], [89]. A solution containing desired concentration of polysulfone (PSF) and sodium hydroxide (NaOH) in NN-dimethyl formamide (DMF) was electrospun into the nano-fibrous membrane.

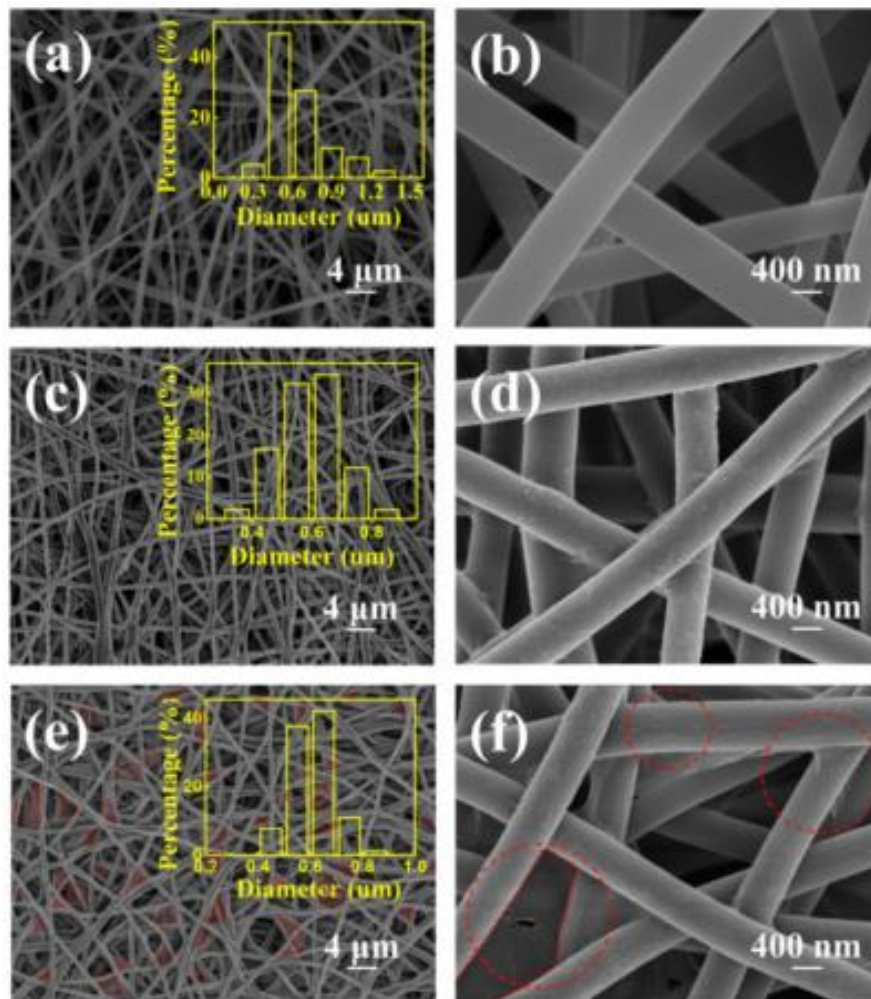


Figure 6. SEM images showing smooth fibers of PAN (a,b), roughened PAN/APAN fibers (c,d), PAN/APAN/GO fibers (e,f) [87]

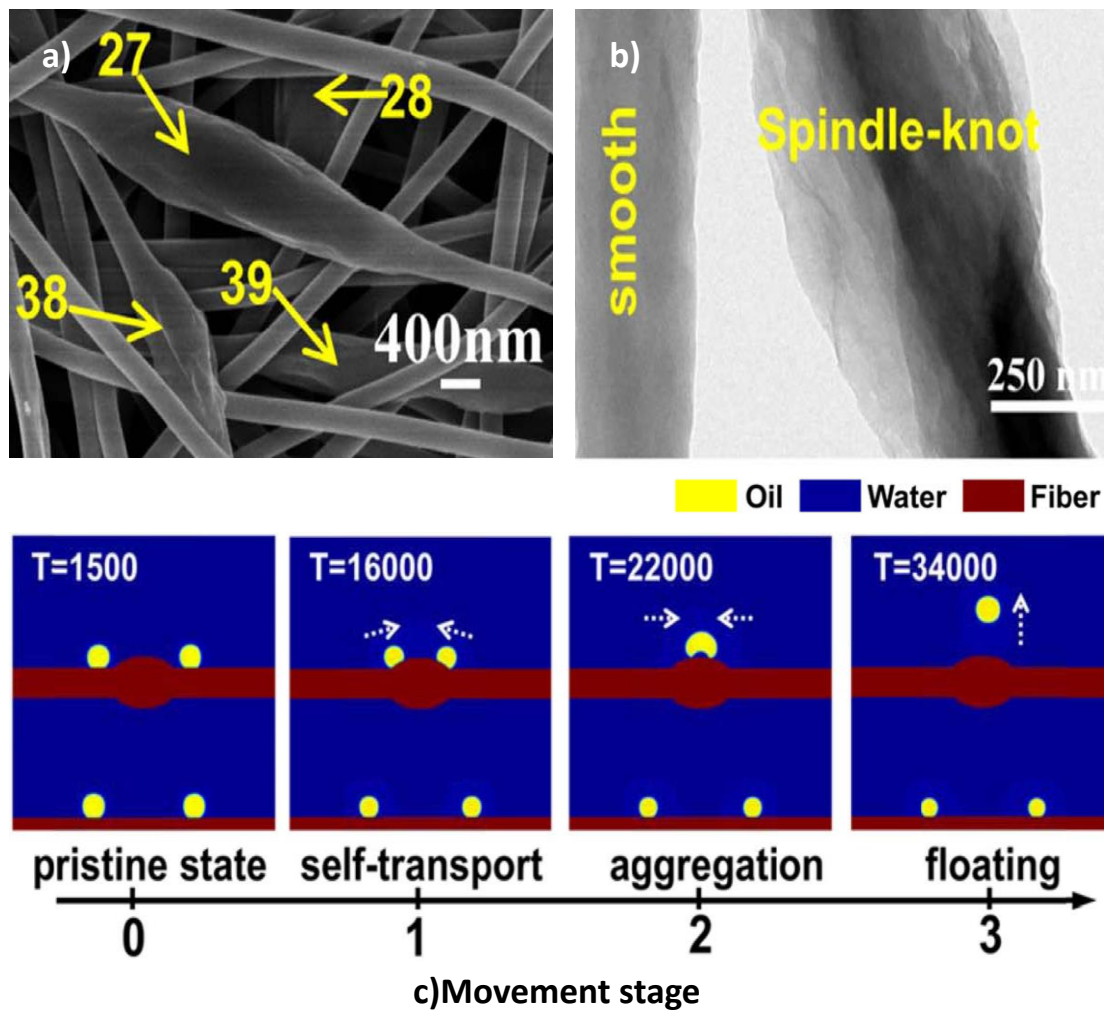


Figure 7. Spindle knotted PAN/GO membrane, a) SEM image, b) TEM image, c) mechanism of demulsification of oil in water emulsion

Later m-phenylenediamine (MPD) (aqueous) followed by 1,3,5-Benzenetricarbonyl chloride (TMC) (in hexane) was applied to form a thin polyamide (PA) layer on the electrospun membrane. SEM analysis indicated that the incorporation of NaOH decreases the diameter of fibers. The contact angle measurements showed that polysulfone membrane modifications through NaOH and PA decrease the water contact angle from hydrophobic to the super-hydrophilic character which was mainly due to a decrease in fiber diameters because of modification.

Oil stability was investigated for the pristine and modified membrane. It was found that the modified membrane remained stable throughout the oil immersion test while the pristine membrane dissolved completely in oil, indicating strong oil stability due to the modification. Another study utilized [90] polylactide (PLA) blend with biocompatible polyester, P34HB in a ratio of 30:70 and 50:50 to develop hydrophilic membrane. The blend polymer was dissolved in a mixture solvent of dichloromethane and ethanol to make reaction solution, which is then electrospun at 20kV into nanofiber mat, further dried under vacuum. The morphological study under SEM figured out that blending with polyester decreases the surface porosity and diameter of the original PLA. Characterization techniques such as were used to check the crystallinity and chemical composition of the synthesized membranes. XRD and FTIR results confirmed that in the absence of polyester, crystallization was not significant while the blending with polyester results in presence of diffraction peak and evolution of absorption band at higher wave number. Water contact angle measurements revealed that the pristine PLA membranes were completely hydrophobic with WCA of 138.5°. When the blending was carried out, the above situation

changes totally, and water starts to wet and permeate through the blend membrane, resulting in hydrophilicity.

2.6.3 Pore size control in electrospun membranes

Various membranes have been developed through electrospinning route. Although it has been highlighted in different studies that the pore size is directly related to fiber diameter [91], [92]. As the fiber becomes thinner, pore size also gets reduced. Coating electrospun membrane with a hydrophilic constituent has added the benefit of reducing the pore size by effectively blocking the liquid passage area. Ejaz Ahmed et al. [45] used a household iron to hot press electrospun PVDF-HFP membranes in order to reduce the pore size. The same group also used a direct coating of cellulose to increase the hydrophilicity, but it has also reduced the pore size from 1 micron (μm) to 0.3 microns (μm). Stretching the electrospun membrane in uniaxial direction is also recently applied to tailor the pore size [93].

2.7 Proposed work based on the recent studies

Based on the recent studies highlighted in table 2, this work is focused on the development of a hydrophilic-oleophobic type of electrospun membranes for separating oil in water emulsion. The reason for choosing this type is that using this hydrophilic-oleophobic membrane, the chances of fouling by oil are less compared to the oil-wetting class of membranes. Also, the fouled oil is difficult to remove and can cause secondary pollutions when chemical treatments are utilized for the cleaning purpose. Another reason for choosing this class of membrane is the fact that the most common oils are lighter than water and naturally will go to the surface after demulsification. Thus, a hydrophilic membrane

promotes natural flow of water and blocks the dispersed oil. Polyacrylonitrile (PAN) is chosen as a starting material due to its intrinsic properties of hydrophilicity, compatibility with other additives, high chemical, and thermal stability, proven electrospinnability and ease of availability. Pure PAN membranes and PAN membranes blended with nanofillers such as silica and/or graphene oxide have been developed in this study. Graphene oxide is known to be beneficial for improving separation performance by enhancing membrane's antifouling properties while silica (SiO₂), which is a natural hydrophilic additive, is believed to improve performance by making the membrane more hydrophilic. In this work, PAN-based membranes reinforced with GO and SiO₂ are fabricated via electrospinning process. The developed membranes are characterized using different analysis techniques and tested to evaluate their separation performance.

Table 2. Recent work on oil-water separation membranes

Material	Technique	Efficiency (%)	Flux (L.m⁻².h⁻¹)
HPAN/GO[88]	Electrospinning & Hydrolyzation	>99	3500
Glass fiber/SiO ₂ [94]	Coating	>98	-
PAN/SiO ₂ [95]	Electrospinning	-	3596
HPAN[23]	Casting	>99	227

CHAPTER 3

EXPERIMENTAL WORK

3.1 Materials

Polyacrylonitrile (PAN) with a molecular weight (Mw) of 1,50,000 g/mol, N, N Dimethylformamide (DMF) (99.8%), silica nanopowder (SiO₂) with an average particle size of 12nm and sodium hydroxide (NaOH) (98%) were purchased from Sigma Aldrich (USA). Concentrated hydrochloric acid (HCl) (35-37%) and polyvinyl alcohol (99% hydrolyzed) with a molecular weight (Mw) 89,000-98,000 g/mol was also provided by Sigma Aldrich (USA). Solid Graphene Oxide (GO) and highly concentrated (5mg/ml) graphene oxide suspension in water with flake size in the range of 0.3 to 0.7 microns (μ) and with carbon/oxygen ratio of 4:1 was purchased from graphene supermarket (USA). All chemicals were utilized as received without any further pretreatment. Deionized (DI) water was obtained from Millipore Milli-Q water purification system and used for purposes such as rinsing, cleaning, and dilution during this study.

3.2 Fabrication of electrospun membranes

Fabrication of nanofiber membranes were carried out using Nanon-01A (MECC Japan) electrospinning setup comprising a power supply capable of providing high voltages of up to 30kV, a syringe pump capable of obtaining a feed-rate of up to 99.9 ml/h, an aluminum

drum collector which can rotate at high rotational speeds of up to 3000 rpm and a closed chamber (figure 8).



Figure 8. Electrospinning setup, Nanon 01A

3.2.1 Electrospinning of PAN membrane

Electrospinning dope solutions were prepared by dissolving 7, 8, 10 and 12 percent of polyacrylonitrile (PAN) by weight in dimethylformamide (DMF) by constant stirring for 24 hours at 60°C and 500rpm using magnetic stirrer equipped with a temperature controller (Thermo scientific, USA). After complete dissolution, some time was allowed at ambient conditions to completely remove the dispersed air bubbles. Homogeneous solutions were then loaded into plastic syringes (locally procured) of 10ml capacity and then electrospun at various combinations of voltages, feed-rate, needle size, spinnret speed, collector rotation while keeping other parameters such as spinnret-to-collector distance, temperature and relative humidity fixed to 15 cm, 25 °C and 80% (table 3). After electrospinning, mats were carefully peeled off from the aluminum foil which was previously wrapped on the collector to ease removal (figure 9). Mats were then cut in reasonable sizes and dried in a conventional oven at 80°C.

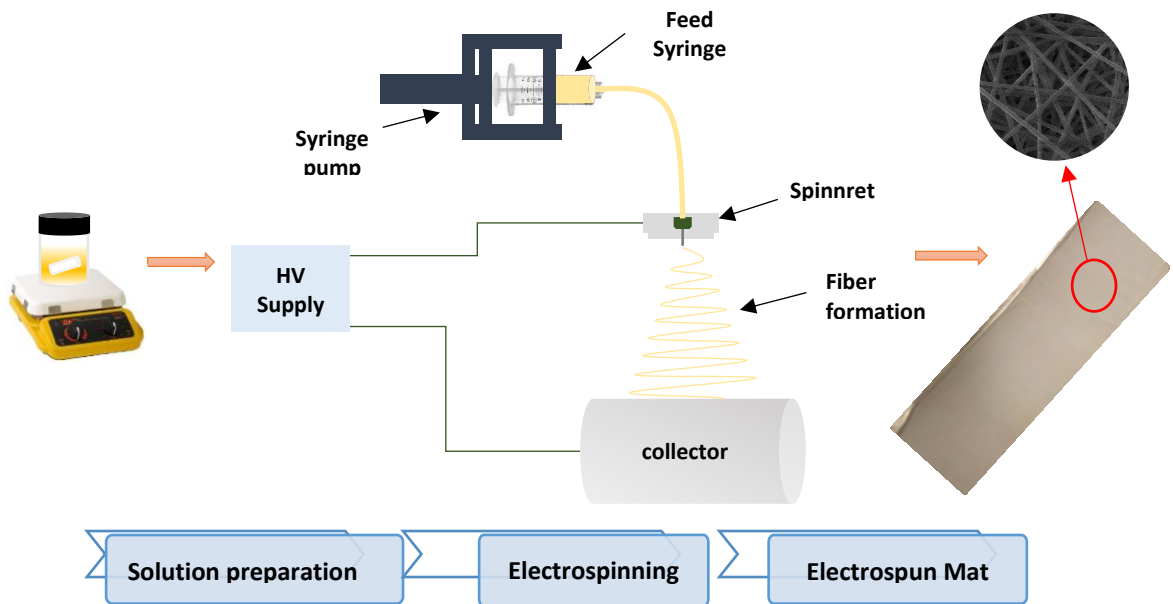


Figure 9. A schematic of electrospinning of PAN based membrane

Table 3. Composition of Pure PAN-based membranes

Composition	Electrospinning Parameters				
	Voltage (kV)	Flowrate (ml/h)	Spinnret speed (mm/s)	Collector rotation (rpm)	Needle size (gauge)
12wt% PAN	20	1	70	300	21G
10wt% PAN	20	1	70	300	21G
10wt% PAN	20	1	70	0	21G
10wt% PAN	20	1	50	0	21G
10wt% PAN	18	1	50	0	21G
10wt% PAN	20	0.8	50	0	21G
10wt% PAN	20	1	100	0	21G
8wt% PAN	20	1	70	0	21G
8wt% PAN	20	1	70	1000	21G
8wt% PAN	20	1	70	300	21G
8wt% PAN	20	1	70	300	18G
7wt% PAN	20	1	70	300	21G

3.2.2 Electrospinning of PAN-Composite membranes

PAN, PAN-SiO₂, PAN-GO and PAN-GO-SiO₂ hybrid membranes were prepared by first dissolving desired amounts of polyacrylonitrile (PAN) in dimethylformamide (DMF)

through vigorous stirring for 24h at 60°C. Silica (SiO₂) and/or graphene oxide (GO) were then separately dispersed in dimethylformamide (DMF) with the aid of ultrasonication for 6h followed by mixing with already prepared PAN solution through vigorous stirring for another 12h such that homogeneous solutions of PAN-SiO₂, PAN-GO, and PAN-SiO₂-GO are formed with total concentrations of 8% by weight in DMF. The resultant dope solution compositions are given in table 4.

Table 4. Electrospinning dope composition of composite-hybrid membranes

Sample designation	Composition
PAN	PAN
PAN-4SiO ₂	PAN+4wt% SiO ₂
PAN-7.5SiO ₂	PAN+7.5wt% SiO ₂
PAN-11SiO ₂	PAN+11wt% SiO ₂
PAN-0.5GO	PAN+0.5wt% GO
PAN-1.5GO	PAN+1.5wt% GO
PAN-4GO	PAN+4wt% GO
PAN-1.5GO-7.5SiO ₂	PAN+1.5wt% GO+7.5wt% SiO ₂

Electrospinning of solutions containing different ratios of nanofillers was conducted at an applied voltage of 20kV to ensure stability. The other process parameters such as feed rate, spinnret to collector distance, collector rotation, spinnret speed, needle size, and temperature were kept constant to 1.0ml/h, 15cm, 300rpm, 70mm/s, 21G and 25°C respectively. Aluminum foil was wrapped around the collector to ease the removal of

electrospun mats. After electrospinning, mats were removed carefully and dried in a conventional oven at 80°C for the removal of the solvent.

3.3 Hot pressing of electrospun membranes

After electrospinning, membranes were pressed using household iron for easy handling and dimensional stability [96]. The surface temperature of the hot surface of the iron was 130°C as determined by placing thermocouples at three different places. For pressing, membranes were sandwiched between two A4 sized papers and hot iron was moved from one end to another for 1-2 minutes to avoid any cause of thermal degradation.

3.4 Exposure to solvent vapors

PAN-based membranes were exposed to the vapors of dimethylformamide (DMF) to see the effect on pore size. Initially, oven dried polyacrylonitrile (PAN) membrane which was electrospun using 8% by weight PAN in dimethylformamide (DMF), was cut into smaller pieces and then four samples were exposed to the vapors of solvent. DMF was first heated in a glass container at 100 °C on a hot plate and then the samples were exposed to DMF vapors for different durations of 0.5, 1, 2, and 3 minutes. After the defined exposure period, samples were then immediately rinsed with deionized water several times and dried at ambient conditions.

3.5 Hydrolyzation of PAN-based membranes

Polyacrylonitrile based membranes were hydrolyzed to improve the hydrophilicity. Samples were cut into reasonable sizes and then placed into glass containers. Already

prepared sodium hydroxide (NaOH) solution in deionized water (DI) with 3M (molar) concentration was then added slowly to this container and then the samples were left in fully immersed conditions for different time periods of 1h, 3h, and 5 h. After the exposure period, samples were rinsed with DI water to remove any residual NaOH and then immersed for 0.5h in 2 M (molar) hydrochloric (HCl) acid solution to neutralize the NaOH treated samples and to complete the hydrolyzation reaction. Samples were then again rinsed with DI water multiple times until all the residuals are free from the membranes and then left overnight at ambient conditions for complete drying.

3.6 Direct coating of GO-hydrogel

PAN-based membranes were subjected to direct coating of polyvinyl alcohol (PVA) and graphene oxide (GO). First, the solution containing 0.5wt% PVA and 0.5mg/ml GO in DI water were separately prepared and then mixed together. The membrane samples were then immersed in this prepared solution for 1-3 hours exposure period at ambient conditions. Water rinse multiple times and then dried at 25°C overnight.

3.7 Characterization of electrospun membranes

3.7.1 Morphological examination

The samples were evaluated for morphological features using high-performance field emission scanning electron microscope (FESEM) (LYRA-3, TESCAN, Czech Republic). It is a high resolution, dual beam FESEM equipped with focused ion beam. Prior to examination, samples were sputter coated with gold for 40 seconds using ion coater (JFC-1100, JEOL, USA) to avoid charging associated with non-conductive materials.

Transmission electron microscopy (TEM) is among the best tools to see the individual fiber surface. JEM-2100F (JEOL, USA) TEM was used to obtain high magnification image of PAN-based fibers. Before TEM analysis, samples were prepared by depositing a single layer of electrospun fibers by placing 150 mesh copper grids directly on the rotary collector and subsequent electrospinning for 2 seconds.

3.7.2 Fourier transform infrared spectroscopy

Fourier transform infrared spectroscopy (FTIR) was carried out using Nicolet 6700 (Thermo scientific, USA) infrared spectrometer, on both bare and modified PAN-based membranes to characterize for the functional groups. An overall range of 4000-600 cm^{-1} , was used in the transmittance mode to get the spectrum. Measurements were performed for many times to get repeatability of results which were then evaluated for further characterizations.

3.7.3 Wetting behavior

The membranes were analyzed for wetting behavior through contact angle measurements under sessile drop method using optical contact angle measurement goniometer (DM-501, Kyowa Interface Science Co. Ltd, Japan). At least three readings were taken for each measurement of water (3 μL) contact angle and then averaged for final results.

For measurement of oil contact angle, samples were placed at the bottom of a transparent container filled with DI water such that samples are fully immersed. Then dichloromethane (DCM) which is heavier than water is used to measure underwater oil contact angle (OCA). At least three readings were taken and averaged for contact angle measurements.

3.7.4 Pore size measurement

The pore size of the fabricated membranes was determined by the expulsion of liquid through gas pressure using capillary flow porometer (3Gzh, Quantachrome Instruments, USA) capable of measuring pore sizes from 500 μ m down to 30nm. Prior to instrument run, membrane samples were cut into 25mm circular shape and then wetted with low surface tension liquid (POROFIL).

3.7.5 Membranes porosity

The porosity of the membranes was determined by using the density of the electrospun membrane and bulk density of the precursor powder according to the following equation [97], [98].

$$P\% = 1 - \frac{\rho_e}{\rho_p} * 100$$

Where P%: Porosity, ρ_e : density of electrospun membrane, ρ_p : bulk density of precursor powder

For porosity calculations, first, the dimensions of the membrane such as length, width, and thickness were calculated with the aid of a ruler and low force (0.01N) digital measuring system (Litematic VL-50, Mitutoyo, Japan) to calculate the total volume. Followed by measuring the weight of the membrane samples.

3.7.6 Tensile testing

Tensile testing of nanofiber membrane was done to determine any changes in mechanical properties due to addition of nano fillers. Membranes with improved mechanical behavior can be helpful for easy handling and reusability. Tensile testing was carried using bench-top tensile testing instrument (ElectroForce 3200) and a constant strain rate of 0.08 mm/sec was selected in accordance with ASTM D 1822.

3.8 Separation of oil and water emulsion

To evaluate the separation behavior of the prepared membranes, an oil in water emulsion, stabilized with surfactant (SDS) (10% of lubricating oil) was prepared using 2000ppm lubricating oil in deionized water while stirring at high speeds of 7000rpm for 1 hour.

Membranes were fixed in dead-end cell consisting of an open-ended beaker and a flask. A constant feed height was maintained throughout the course of the experiment such that a pressure of 0.1bar is exerted due to the height of liquid column without applying any external force. Separation testing was carried out for at least three cycles with intermediate rinsing with water and ethanol.

After separation experiment, permeates were evaluated using total organic carbon analyzer (TOC) (TOC-VCHS, SHIMADZU, Kyoto, Japan) and compared with the original concentrations of the feed emulsion to determine the rejection percentage and membrane's separation efficiency [97]. Optical micrographs and digital images were also taken to analyze the separation performance.

CHAPTER 4

RESULTS AND DISCUSSION

4.1 Parametric study

In this section, the effect of various parameters used during electrospinning of polymers is discussed. Electrospinning dope solutions containing polyacrylonitrile in different concentrations are utilized and membranes with finer fibers together with the smallest density of defects will be chosen for later studies. Here it should be noted that the control of pore size is directly related to the fiber diameter, finer fibers ensures smaller pore size, thus improves separation performance [99], [100].

4.1.1 Effect of voltage

PAN-based membranes were fabricated through electrospinning using various combinations of process parameters. Change in fibrous morphology and diameter of fibers was evaluated using scanning electron microscopy. It is clear from the previous work that the change in process parameters causes a significant change in resultant fibrous properties. A change in voltage can cause an increase or decrease in the fiber diameter or may cause drop instead of continuous fibers. In this study, it is found that there is a narrow range where one can obtain continuous fibers. Above or below this threshold limit, intermittent stops could be observed. When applied voltages varied from 18 to 20 kV for constant solution composition, spinnret or collector speed, needle size and spinnret to collector distance, it was noticed that at higher voltage, finer fibers resulted (figure 10 a-d). This

decrease in fiber diameter could be attributed to the increase in charge repulsion due to an increase in voltage causing more stretching during fiber formation and collection. Beyond this range, unstable jets were initiated directly from the tip or inside of the needle, resulting in the formation of bead defects due to an increase in the ejected volume of solution. Below this threshold range, continuous fibers could not be obtained.

4.1.2 Effect of flow rate

Due to inherent flexibility in electrospinning process, there are various parameters which can be played with to achieve the required fibrous characteristics. Among these parameters, the flow rate of the feed solution has significant importance. An increase in the flow rate could increase the amount of polymer in the resultant fibers. This increase in the feed per unit time increases the amount of polymer in the fiber jet. An intermediate concentration of 10% by weight of PAN solution in DMF (solvent) was selected to study the effect of solution feed rate on resultant fibrous morphology. The first step towards this study was to find the minimum flow rate that can ensure continuity in the fiber formation. We found that the threshold limit is 0.8ml/h for this solution composition when other parameters were fixed to some defined values. Below this limit, dripping or intermittent stops were noticed. Thus, we carried out the high magnification SEM examination (figure 10 e-h) of varied flowrate between 0.8ml/h to 1.0ml/h. It can be observed that at higher flow rate, the mass flow rate increases, which also increases the fiber diameter. Also, by observing the magnified image, not only the fiber diameter decreased, but fiber distribution also became narrower at a feed rate higher than 1.0ml/h.

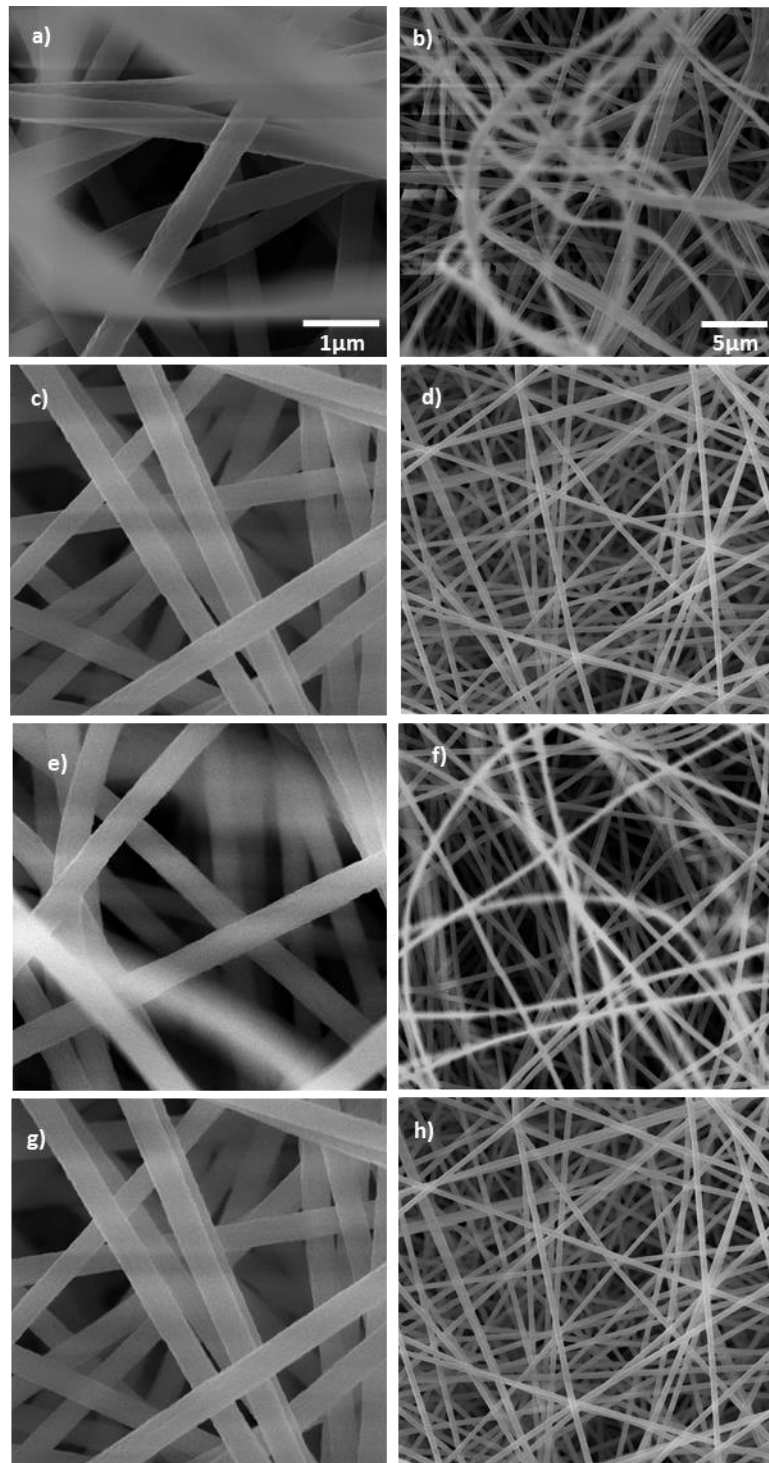


Figure 10. Effect of voltage on PAN fiber: a-d, a & b) 18kV, c & d) 20kV, Effect of flowrate on PAN fiber e-h, e & f) 0.8ml/h, g & h) 1ml/h

This narrowness and uniform distribution could be the main reason that most of the studies used the same flow rate. Thus, based on these observations, we used a fixed flow rate of 1.0ml/h in the following sections.

4.1.3 Effect of spinneret speed

Although there are many studies in this area and much work have already been done. It had noticed that there is a lack of studies which focuses on how the spinneret speed can affect the electrospinning process and the resultant fibrous properties. Due to this reason, we strived to investigate the effect of spinneret speed (the travel speed of spinneret/feed needle in the x-direction). PAN-based solution containing 10% PAN by weight in DMF was electrospun at varying speeds of 50mm/s, 70mm/s, and 100mm/s while the other parameters remained fixed. The fabricated fibrous mats were then analyzed under the SEM and high magnification images were captured (figure 11). It can be noticed from the SEM images that there is an influence of spinneret speed on resultant fiber morphology. The fiber diameter got reduced (420nm to 270nm) when the spinneret speed was increased from initial 50mm/s to 70mm/s. It also observed that when the speed was further increased to 100mm/s, surprisingly, the diameter again started to increase (402 nm). It can be said that the initial decrease in fiber diameter was due to the greater stretching during fiber deposition on the collector. This stretching increased further at a higher speed of 100mm/s. But instead of further decrease, the fibers became thicker which could be because of greater instability during fiber formation at much higher speeds.

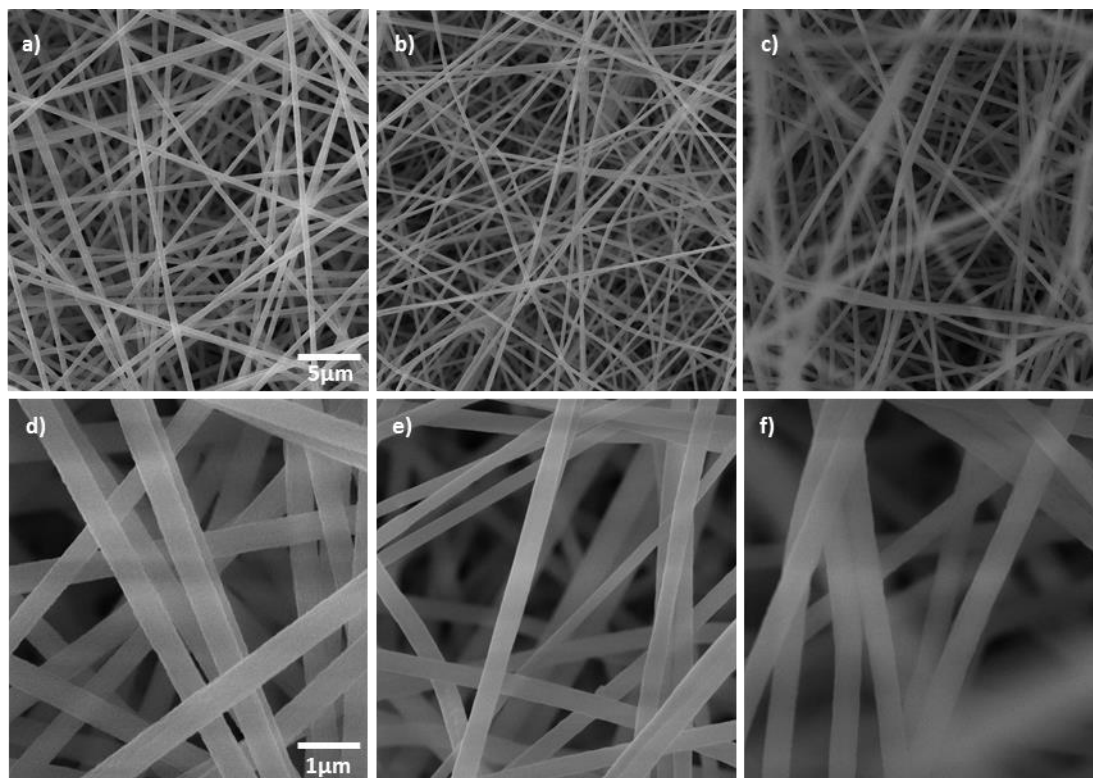


Figure 11. Effect of spinneret speed on PAN fiber, a & d) 50mm/s, b & e) 70mm/s, c & f) 100mm/s

4.1.4 Effect of polymer concentration

Due to the reason that the polymer concentration could play a major influence on final fiber morphology, the electrospinning using four different concentrations of polyacrylonitrile (PAN) was conducted. We had chosen 7%, 8%, 10% and 12% PAN concentrations and analyzed them for morphological characteristics.

It could be observed from the SEM micrographs (figure 12) that an increase in the fiber diameter can result from an increase in polymer concentration. This increase in fiber diameter observed to be more than 200% from initial 167 nm at 7wt% to 410 nm at 12% PAN concentrations. With an increase in the polymer concentration, the number of bead defects also reduced. This reduction in beads formation could be mainly attributed to the increase in viscosity and increased chain entanglements with the increase in polymer concentration [97]. At 7%PAN, we can see many bead-fiber combination morphologies, which could be because of the insufficient viscosity due to which, chain entanglement got reduced and caused the polymer jet to broke up due to lower viscoelastic forces in comparison to the larger repulsive forces. As the concentration increased beyond 7%PAN, the resultant morphology changed to fiber dominant and become more uniformly distributed.

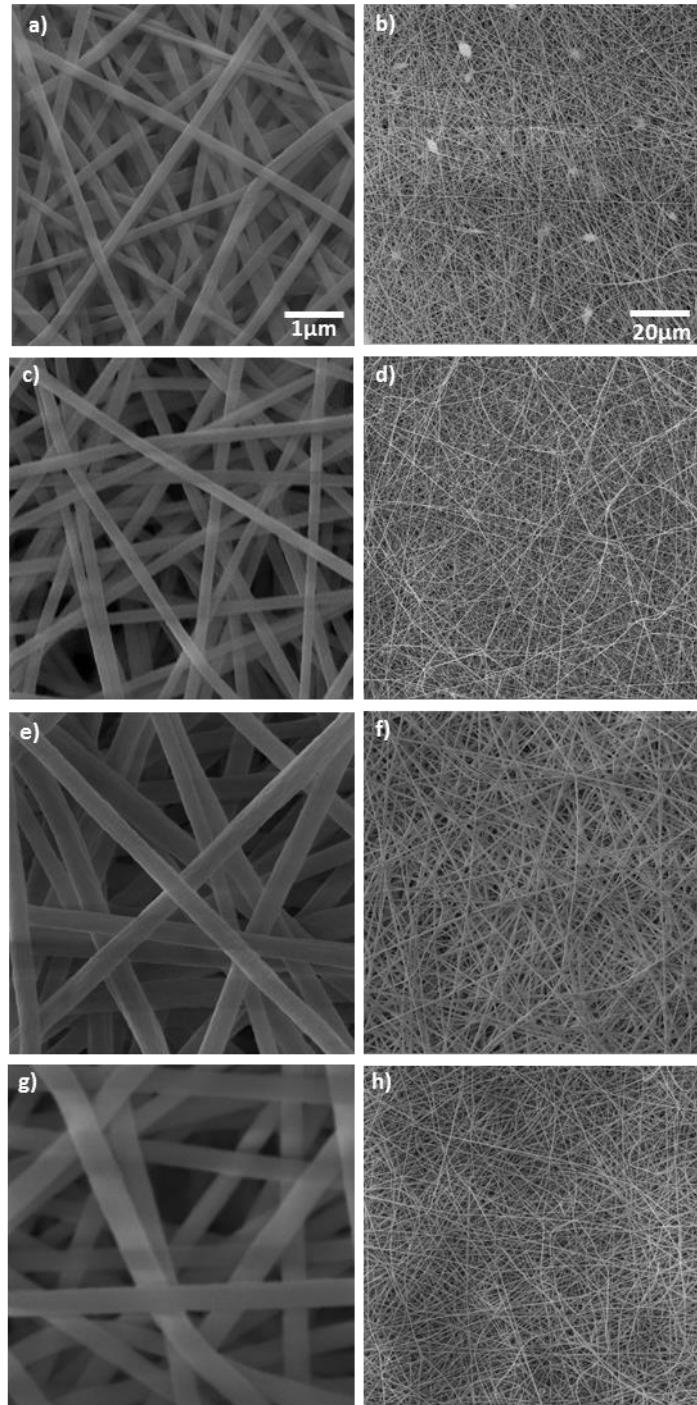


Figure 12. Effect of concentration on PAN fiber, a & b) 7wt% PAN, c & d) 8wt% PAN, e & f) 10wt% PAN, g & h) 12wt% PAN

4.1.5 Effect of rotational speed

Electrospinning process has mainly two types of physical movements; horizontal movement of the spinneret and rotation of the collector drum. We have already discussed the effect of spinneret speed in the previous section. The effect on fibrous properties due to a collector rotation are highlighted in the next section.

The collector is the portion of electrospinning setup, where the fibers from the spinneret are collected in the form of a mat. The rotational speed of this collector can affect the resultant fibrous morphology. After going through the previous works, we found that there is lack of work that discusses the effect of rotational speed.

In this work, we tried different combinations of rotational speed for pure PAN composition. The 8% by weight solution was electrospun at 0, 300, 500 and 1000 rpm and morphological examination was carried out using SEM. It can be seen from the SEM images (figure 13) that the increase in rotational speed causes the fiber diameter to decrease from initial 305 nm (0 rpm) to 230 nm (1000 rpm). This decrease in fiber diameter could be mainly because of the increase in fiber stretching with increased rotation during deposition. This increased stretching could also cause instability in fiber formation after some threshold rotational speed. We have noticed from our study that this threshold limit is 300rpm for 8%PAN compositions. After 300rpm, the deposition of fibers shows instability. Thus, we had chosen 300rpm for our later studies.

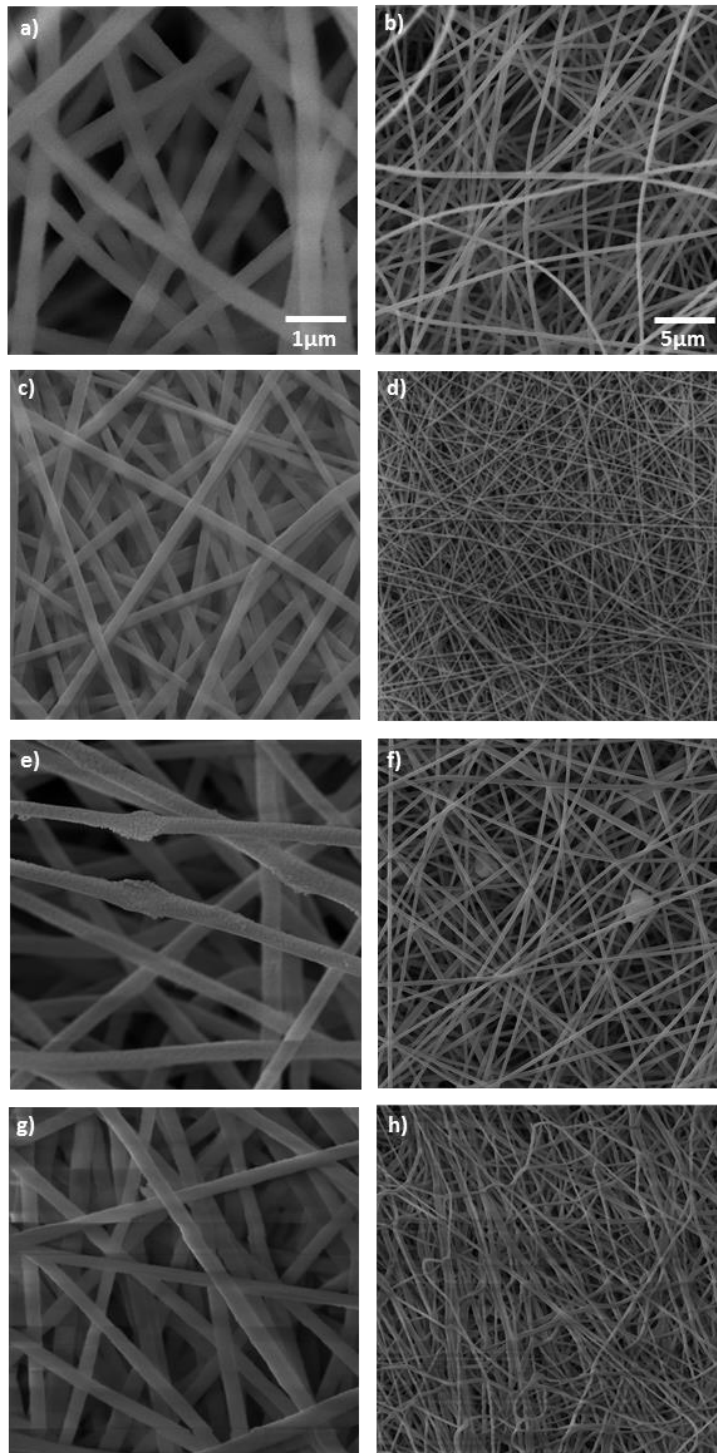


Figure 13. Effect of collector rotational speed on PAN fiber, a & b) 0 rpm, c & d) 300 rpm, e & f) 500 rpm, g & h) 1000 rpm

4.1.6 Effect of needle size

The size or diameter of feed needle attached with the spinneret is also very important factor in electrospinning process. It can affect the behavior of fiber formation on the collector. Considering the importance of this factor, we had also studied the effect of needle size. Although the previous work suggested that the effect of needle size is little more controversial, where some researchers [101] said that there is no correlation between the fiber diameter and the needle size while the others mentioned that by increasing the size of needle, the fiber diameter will also be increased [102]. We had electrospun 8% PAN by varying the needle size from 18G (0.8mm ID) to 21G (0.6mm ID). It is cleared from the SEM images (figure 14) that the increase in needle gauge caused the diameter of fibers became smaller and fibrous morphology seems to be more uniform. The reason for this effect was clearly explained by Sutasinpromprae et al.[103] and Sencadas et al.[104] that when the diameter of the needle is bigger, there will be easy jet ejection from bottom of the needle, causing jet length to be larger before reaching to the bending instability, thus solvent evaporation will be smaller compared to the case of smaller diameter needles, where the bending instability region will be larger and jet length will be shorter.

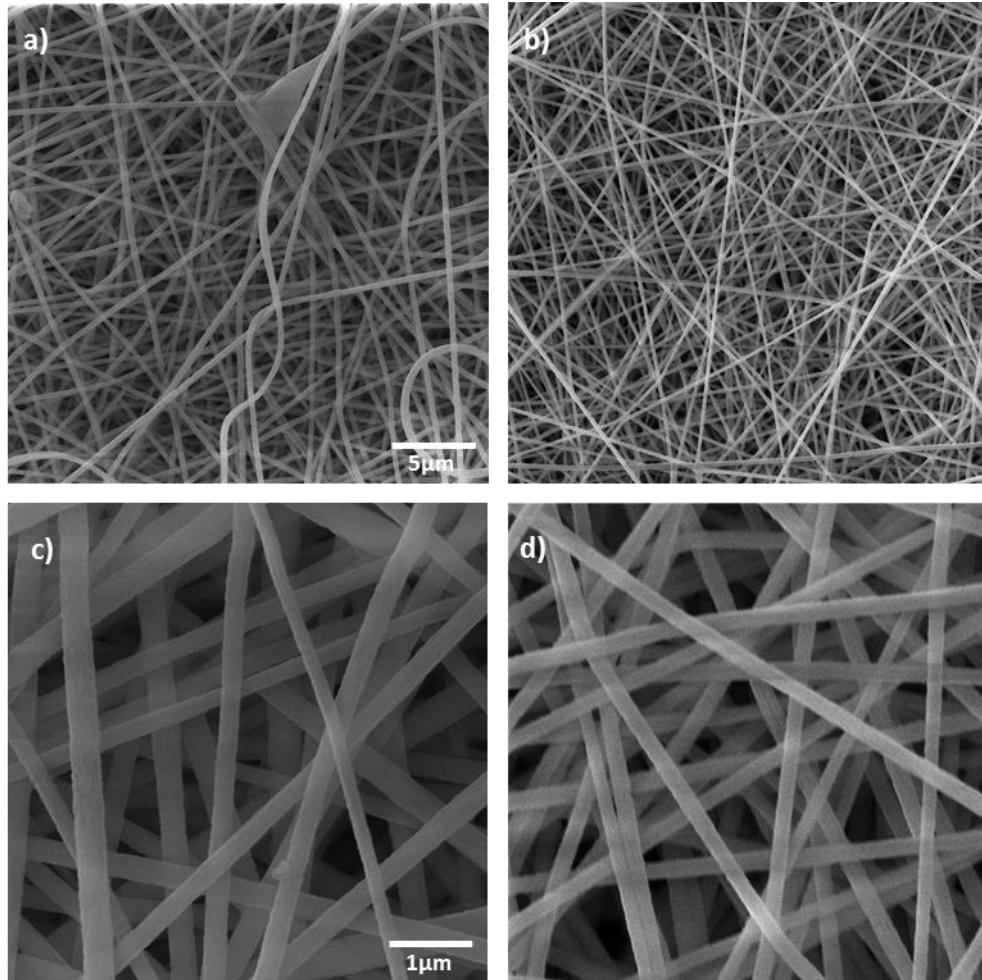


Figure 14. Effect of needle diameter on PAN fiber, a & c) 18G (0.8mm), b & d) 21G (0.6mm)

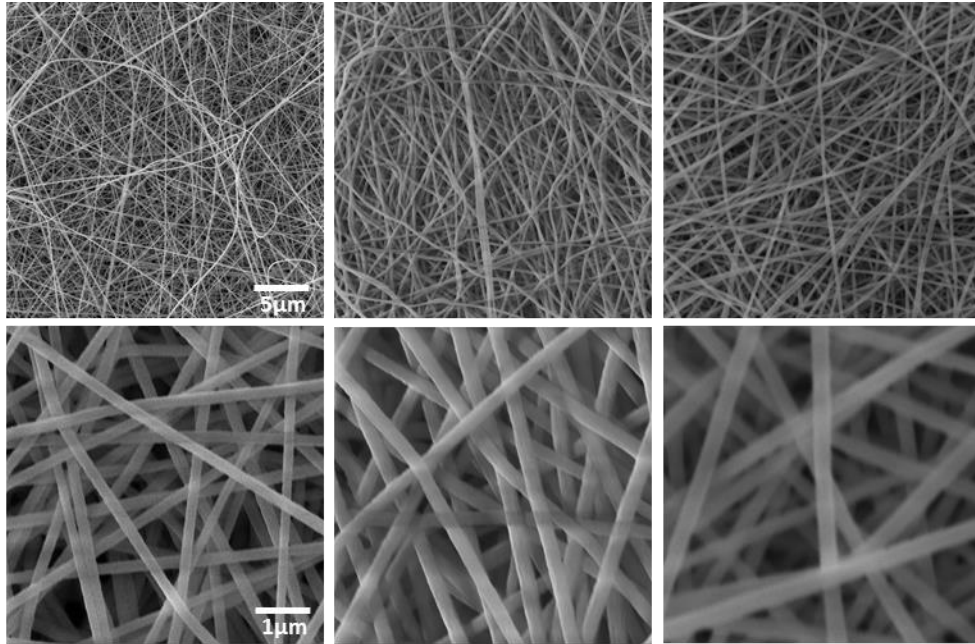
4.2 Hydrolyzation of PAN-based membrane

Hydrolysis of polyacrylonitrile-based membranes is a common method of substitution for nitrile group to more hydrophilic groups. Through partial hydrolysis with sodium hydroxide (NaOH), the nitrile group ($-C\equiv N-$) on the surface of PAN changes to the carboxylic acid group. We had selected PAN-based membrane, fabricated through electrospinning of 8% PAN in DMF for hydrolysis treatment by NaOH. Three molar (3M) concentration of NaOH aqueous solution was selected based on the recent studies [23], [105]. PAN membranes were immersed for 1h, 3h and 5h in 3M NaOH solution at room temperature, rinsed with DI water and then immersed for 0.5h in 2M HCl solution to complete the hydrolyzation reaction.

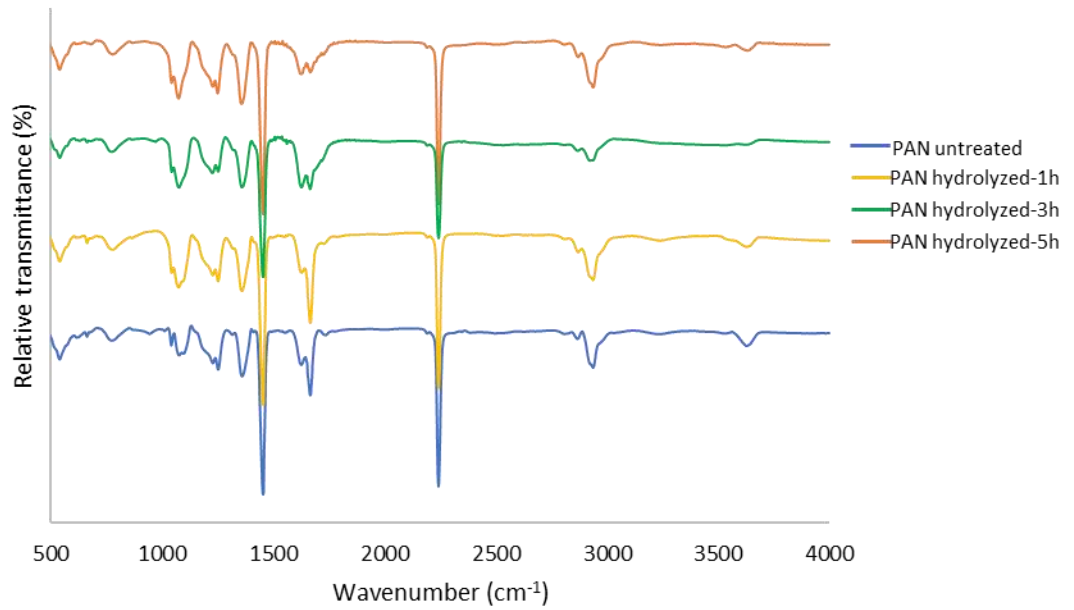
As depicted by SEM images (figure 15 a) the membranes are composed of fibers with continuous randomly oriented entangled structures and are highly porous. It can be observed that the untreated PAN membrane has comparatively smooth fibers with an average fiber diameter of 200 nm. Upon treating with NaOH, the surface of PAN membrane became rougher and rougher with treatment time [23]. This roughness which is a combination of micro-nano features known as a hierarchical structure is believed to be beneficial for separating oil from water as it could allow water to stay inside and keeps the oil from direct contact with the membrane surface by creating water pockets. The treatment with NaOH also caused the swelling of fibers and fiber diameter increased to 270nm at 3-hours hydrolysis while at a longer treatment time of 5-hours, it rose to 300nm. Both increase in roughness and fiber diameter can be well understood by the fact that exposure to harsh conditions causes degradation or corrosion and wear of materials. Thus, exposure

of PAN membrane to NaOH and HCl caused wearing of the surface, together with beneficial effects of incorporating more hydrophilic groups [106], [107].

The surface chemical structure of the treated and untreated membranes was also characterized by FTIR spectroscopic studies (figure 15 b). All the membranes have a common peak at 2243 cm^{-1} , corresponds to stretching vibration band of nitrile group ($-\text{C}\equiv\text{N}-$) for polyacrylonitrile. Treating with NaOH caused the intensity of nitrile peak to be decreased which is evident of hydrolysis. The increase in the intensity of peaks at 1072 cm^{-1} , could be because of stretching vibration of C-O representing the carboxylic acid group, and the reduction in intensity of nitrile group ($-\text{C}\equiv\text{N}-$) stretching vibration at 2243 cm^{-1} , reflects effective conversion of nitrile to carboxylic acid group [88][105].



a) FESEM images of Hydrolyzed PAN membrane



b) FTIR spectra of Hydrolyzed PAN membrane

Figure 15. SEM images of hydrolyzed PAN based membranes (a), FTIR spectra of hydrolyzed PAN based membranes (b)

For a membrane, the pore size is also of significant importance. A membrane should have a pore size that is small enough to successfully block the required component. Porometric study of the hydrolyzed PAN-based membranes was carried out to analyze the effect of NaOH treatment on pore size. Table 5 illustrates the pore sizes of untreated and treated PAN-based membranes. Untreated PAN membrane prepared through electrospinning of 8%Pan solution in DMF, has an average pore size of 1.2 μm . When the PAN membrane was treated with NaOH, the pore size of the membrane was decreased to 0.8 μm . The reason for this decrease in pore size could be the swelling of fibers due to treatment with NaOH. These swelled fibers decrease the pore opening and decrease the pore size [108].

Table 5. Effect of hydrolyzation on the pore size

Immersion time (h)	Pore size (μm)
0	1.2
1	0.9
3	0.8
5	0.8

Wetting characteristics of the NaOH treated membranes were analyzed through the measurements of water and underwater contact angles (figure 16). The untreated electrospun membrane has a water and oil contact angle (underwater) of 15° and 125° respectively. This oil and water contact angles highlight that the PAN electrospun membranes are inherently hydrophilic and oleophobic. Hydrolysis with NaOH caused

enhancement in hydrophilic-oleophobic property, due to the conversion of nitrile group to more hydrophilic groups as already depicted by FTIR spectroscopy. The contact angle for oil underwater was increased to 155° when the electrospun membrane was immersed for 3hour in 3M NaOH solution. Although the water contact angle (captured within 5 seconds of drop placement) was not changed significantly, which might be because of the increased roughness and keeping in view the contact angles were measured immediately within 5 seconds of drop placement. This increased roughness needs time (called dwell time) to allow water to be absorbed.

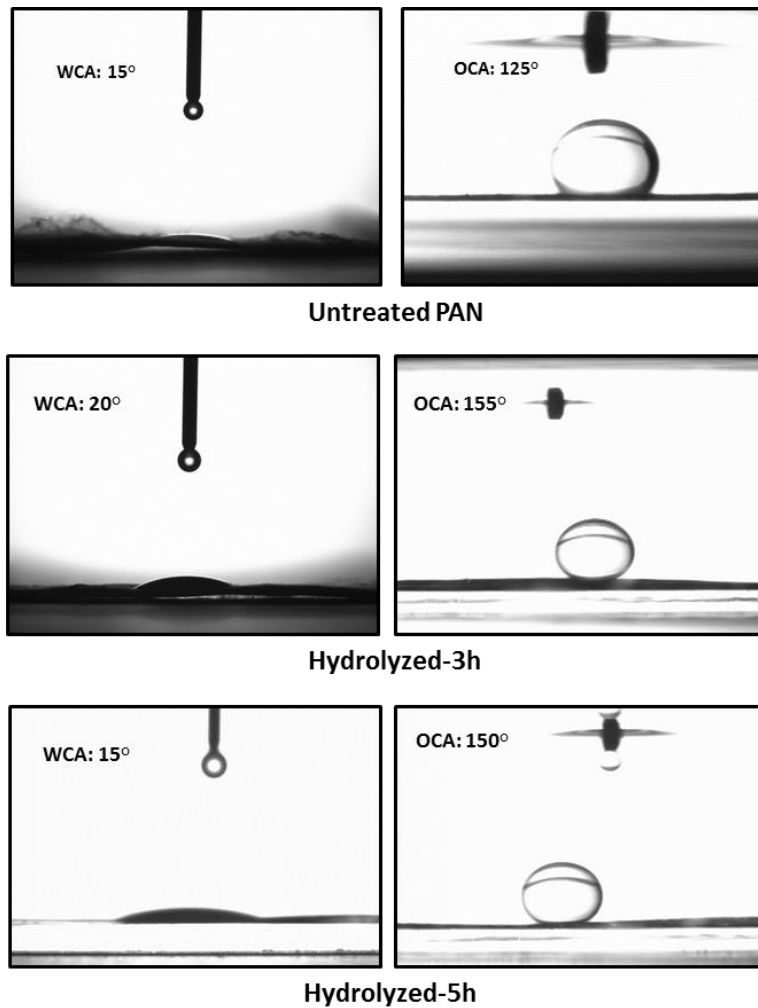


Figure 16. Wetting characteristics of hydrolyzed PAN membranes

The increased in oleophobicity was also depicted by the separation testing. We had used 2000ppm oil in water emulsion for separation testing when the membranes were fixed in the dead-end filtration cell. The separation was carried out under gravity and the height of liquid column was fixed to exert a constant pressure of 0.1bar for the test period. Separation performance of the PAN-based membranes is shown (figure 17). The untreated PAN-based membrane has a onetime separation flux of 2600 L.m⁻².h⁻¹, proving its inherent hydrophilic-oleophobic character. The separation flux of PAN-based membrane increased to 3100 L.m⁻².h⁻¹, for 3h treatment with NaOH. This increased flux with high separation efficiency as depicted by the microscopic (optical) and digital images (figure 17b) of the permeate is because of the highly hydrophilic surface constitution. It should be noted here that the increase in hydrolysis time beyond 3 hours, caused both flux and separation efficiency to be declined. This poor separation performance at higher hydrolysis times, although not very clear from the previous studies, could be attributed to the excessive corrosion of the fibrous surface which might cause smoothening of the fibers and result in low separation efficiency [107].

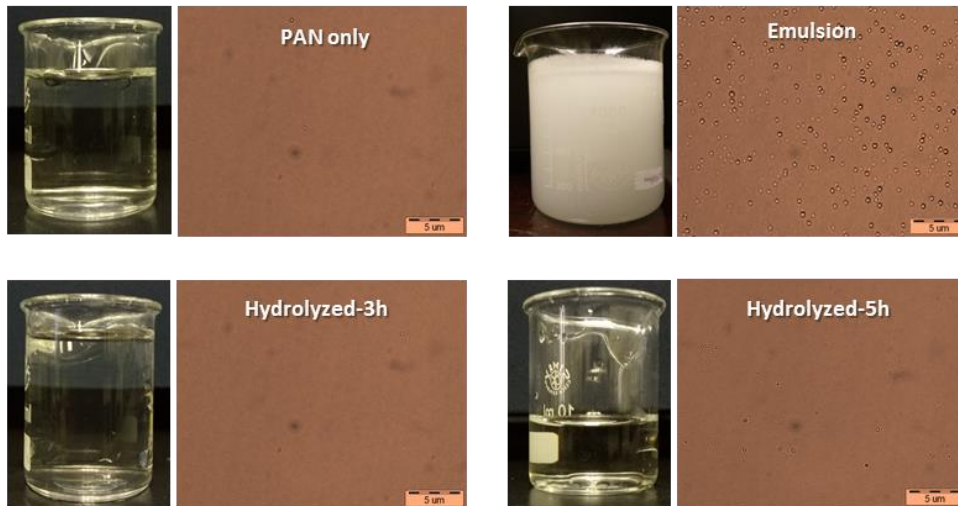
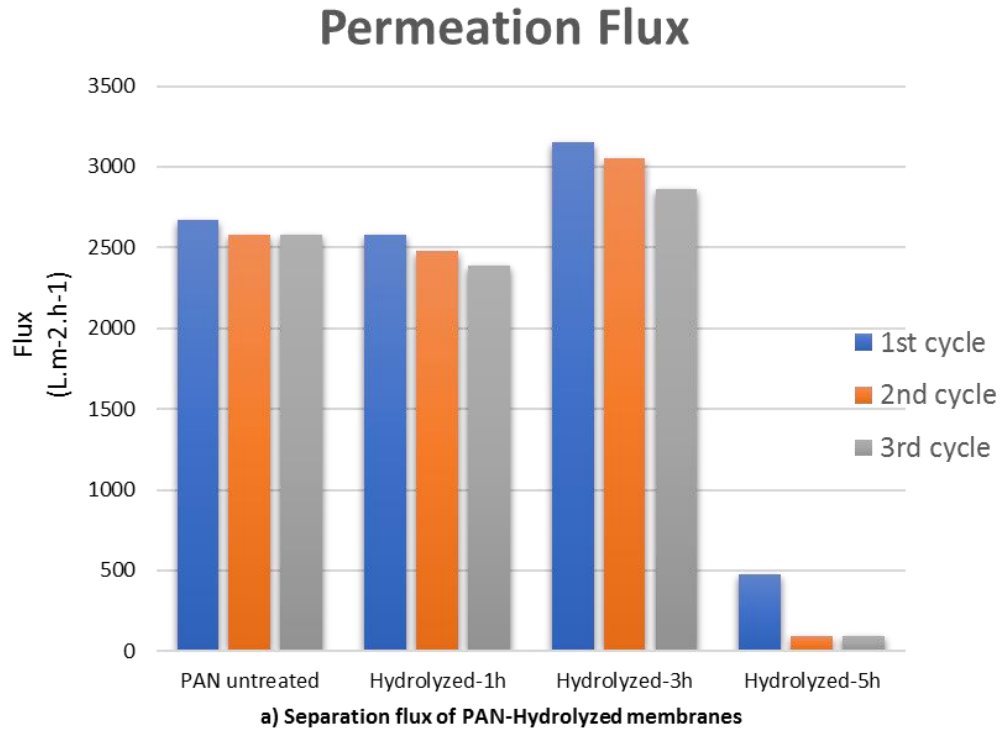


Figure 17. Separation performance of hydrolyzed PAN based membranes, (a) permeate fluxes, (b) separation permeate images

4.3 Direct coating of GO-hydrogel

Here we have reported another approach to enhance the separation performance of PAN-based membranes by depositing a thin layer of hydrogel combined with graphene oxide. The purpose of applying hydrogel here was to act as mortar for GO which acts as building block for coating highly porous entangled electrospun membrane. In this novel approach, 8% PAN electrospun membranes were immersed in a solution containing low concentrations of polyvinyl alcohol (PVA) (0.5wt%) and graphene oxide (GO) (0.5 mg/ml) for different time periods of 1 and 3 hours based on the previously reported work [109]. The aim of the chosen very low concentration was to coat only the surfaces of individual fibers and to avoid the formation of a thin film on the membrane surface to eliminate any detrimental effect on permeate flux. It can be observed in SEM images (figure 18) that at low immersion time of 1 hour, the coating was insufficient to cover the surface of the membrane but only covered some fibers. As the immersion time increased, the coating became more pronounced as can be seen for 3-hour immersing coating. It can be observed that the individual fiber surfaces have some change which can be considered as an evidence for PVA/GO coating while few areas of the membrane surface were also covered with the thin film. The formation of the hydrogel-GO coating is expected to improve the separation performance of PAN-based membrane due to the more hydrophilic and antifouling nature of the coating components [110], [111].

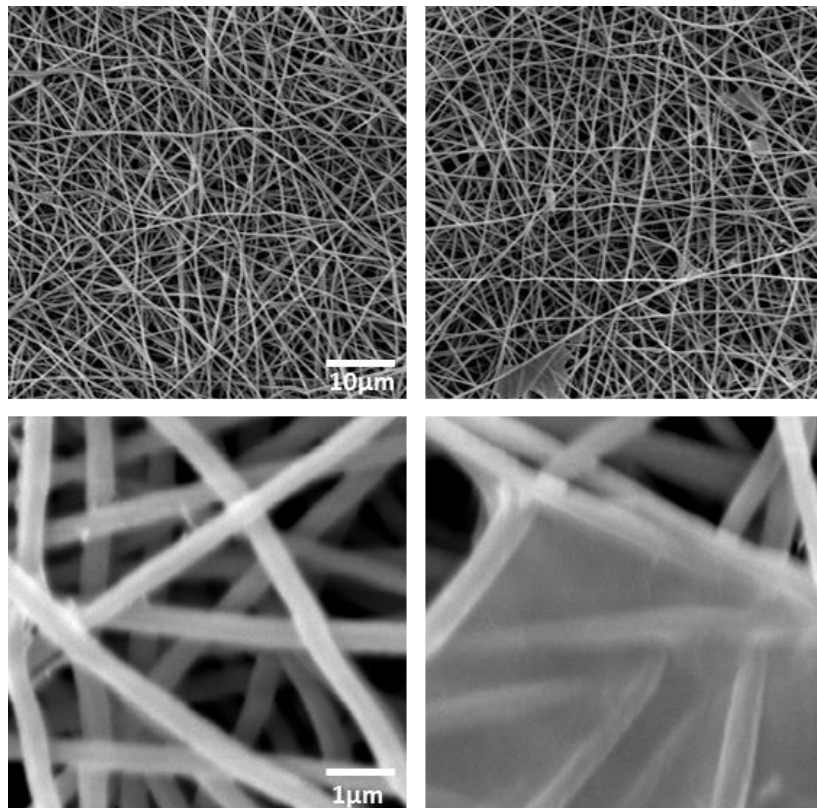
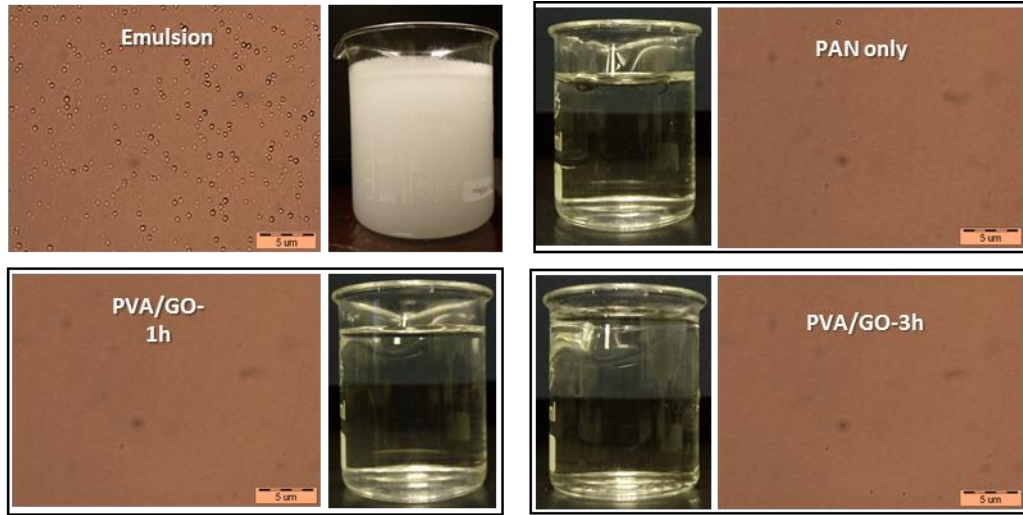


Figure 18. FESEM images of PVA-GO coated PAN



a) Optical microscopic and digital images of the permeates

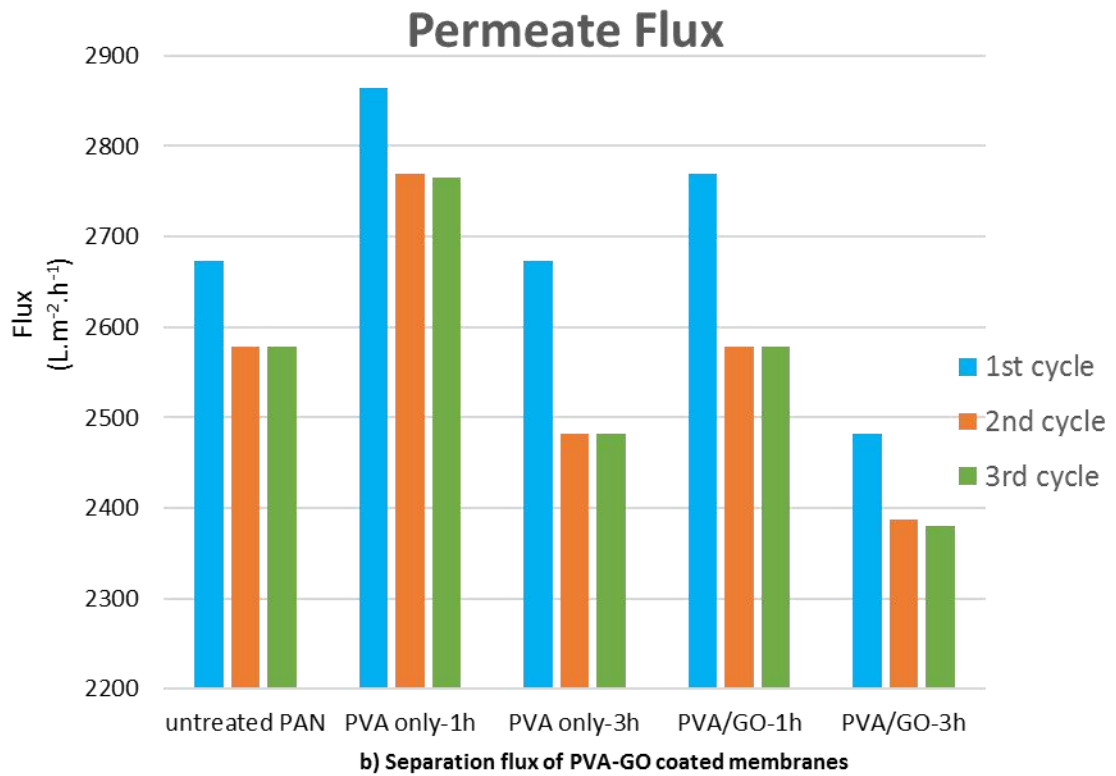


Figure 19. Separation behavior of PVA-GO coated electrospun PAN membrane

Pore size measurements also revealed the successful coating of hydrogel-GO on electrospun PAN membrane. Untreated PAN membrane had a pore size of 1.2 μm , which was reduced to 1.0 μm through immersion for 3-hours. This reduction in pore size depicted that the coating has covered some portion of the porous structure together with the individual fibers, which was expected as it is very difficult to apply coating only at individual fibers of electrospun membrane composed of fibers oriented randomly.

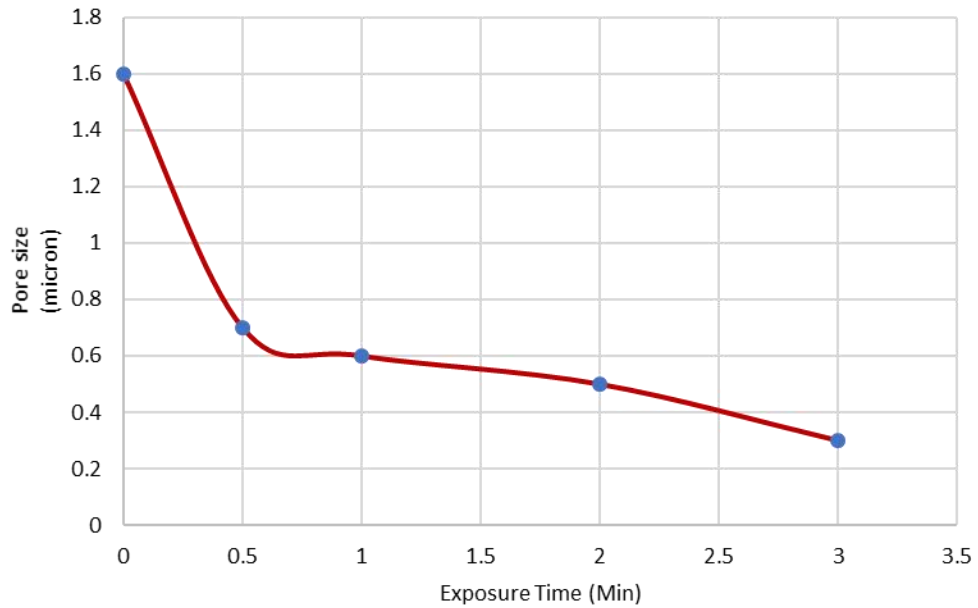
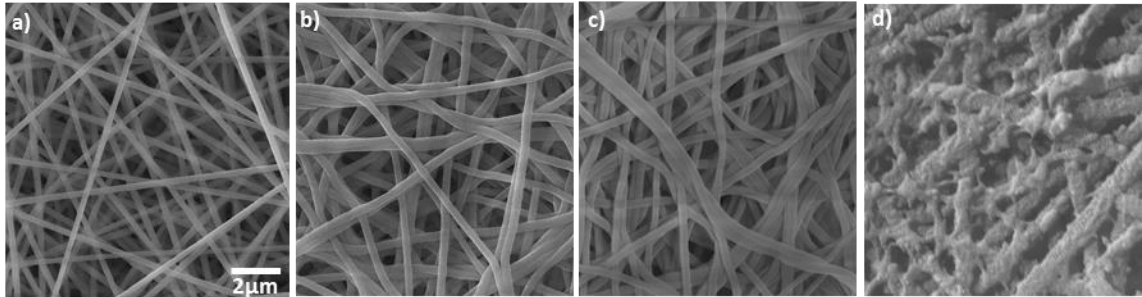
Performance evaluation of PVA-GO modified membranes was conducted through separation testing of 2000ppm of oil in water immersion. It can be revealed (figure 19) that these membranes have good separation characteristics with high separation efficiency as illustrated by optical images of the milky feed and the transparent permeate. Also, the separation flux of these membranes is high, with good flux recovery in multiple cycles of separation testing. Here (figure 19b) we have shown, three cycles for each membrane and the flux recovery is high for 1 hour treated membrane and then decreases.

4.4 Direct exposure to solvent vapors

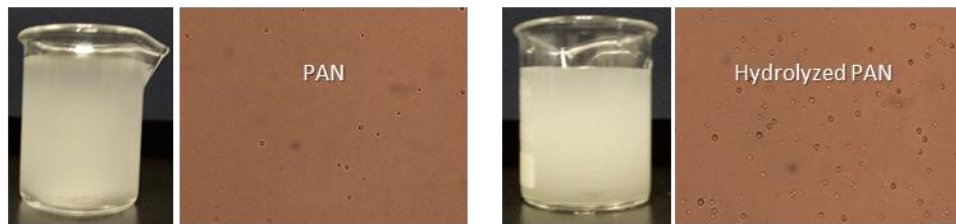
The control of pore size of the membrane is very important, and it depends on the required application. In electrospinning, there is no direct control of pore size but can be indirectly controlled by the fiber size. As the diameter of fibers decreases, the pore size also decreases [112]. Considering the fact that the membranes prepared by electrospinning are mostly microporous, previous studies have used to apply surface coatings to decrease the pore size [45].

Here we had used a novel approach of exposing electrospun membranes to vapors of solvent to reduce the pore size. 8%PAN membrane samples were exposed to the vapors of

dimethylformamide (DMF) at a temperature of 100°C, which is far below the boiling point of DMF (150°C) for different time periods of 0.5 to 4 minutes and expected to have reduced pore openings. Pore size measurements of the exposed membranes from 0.5-3 minutes exposure period are summarized (figure 20e), while above 3 minutes, we observed melting of the membrane samples. It can be observed that there is a significant reduction in pore size with exposure to solvent vapors. At 0.5 minutes exposure, the pore size reduced to 0.7 μm from initial 1.6 μm . With increased exposure period, the pore size was continued to decrease and reached a value of 0.3 microns for 3 seconds exposure period. This decrease in pore size could be because of the merging of fibers and some localized fusion at the intersection points. It is cleared from the SEM images (figure 20 a-c) that the exposure to solvent vapors caused the individual fibers to merge together and reduced the pore size. Based on the reduced pore size, we expected to apply these membranes for separation of oil in water emulsions. Membrane with 0.7 μm pore size with an exposure period of 0.5 minutes was selected for the separation testing. Despite reduced pore size (Figure 20f), the permeate is whitish. This whitish permeate shows that the separation performance is not better than the unexposed membranes discussed earlier. As another proof, we have also exposed 3-hour hydrolyzed PAN-based membrane for the same exposure period of 0.5 minutes and applied for separation testing. As shown in the digital images (figure 20f), the permeate is still whitish, which confirms the previous results for the unhydrolyzed PAN-based membrane. The reason for this poor separation performance is more cleared from the SEM images (figure 20 a-d) of both types of membranes.



e) Effect on pore size due to exposure to DMF vapors



f) Separation performance of PAN and Hydrolyzed PAN membranes exposed to vapors of DMF for 0.5 min

Figure 20. Effect of exposure to DMF vapors on electrospun PAN membrane, (a-d) FESEM images of :(a) 0 min exposure, (b) 0.5min exposure, (c) 3min exposure, (d) 0.5 min exposure on hydrolyzed membrane, (e) Pore size vs time of exposure, (f) separation performance for PAN and hydrolyzed PAN membrane

It can be seen clearly that the solvent exposure results in the destruction of fibrous structure for the hydrolyzed membrane. This destruction of the fibrous structure is believed to be the main cause of poor separation performance.

4.5 Characterization of PAN/PAN-based nanocomposite membranes

Combination of surface chemistry and a hierarchical structure composed of micro-nano features is required for effective treatment of oily waters. An emulsified mixture of oil and water can be separated when passed through a membrane of high hydrophilicity and comparable pore size with surfaced hierarchical structure. We have developed PAN-based membranes with different concentrations of graphene oxide and silica. The appearance of the membranes after adding inorganic fillers was also changed (figure 21-right). The whitish colored pure PAN-based membrane became greyish with the addition of graphene oxide (GO) which proves the uniform distribution of GO in the polymer solution. With the addition of silica (SiO₂), there was no significant change in membrane's appearance and it remained the same whitish in color which could be because of the original appearance of the silica powder. FESEM images (figure 21-left) of the pristine PAN, composite membranes composed of PAN-GO and PAN-SiO₂ and hybrid membrane composed of PAN-GO-SiO₂ are shown. It is cleared from the high magnification SEM images that the structure became rougher when polyacrylonitrile was blended with either graphene oxide or silica alone or in combination. All the membranes are composed of entangled randomly oriented fibers forming highly porous 3D non-woven structure.

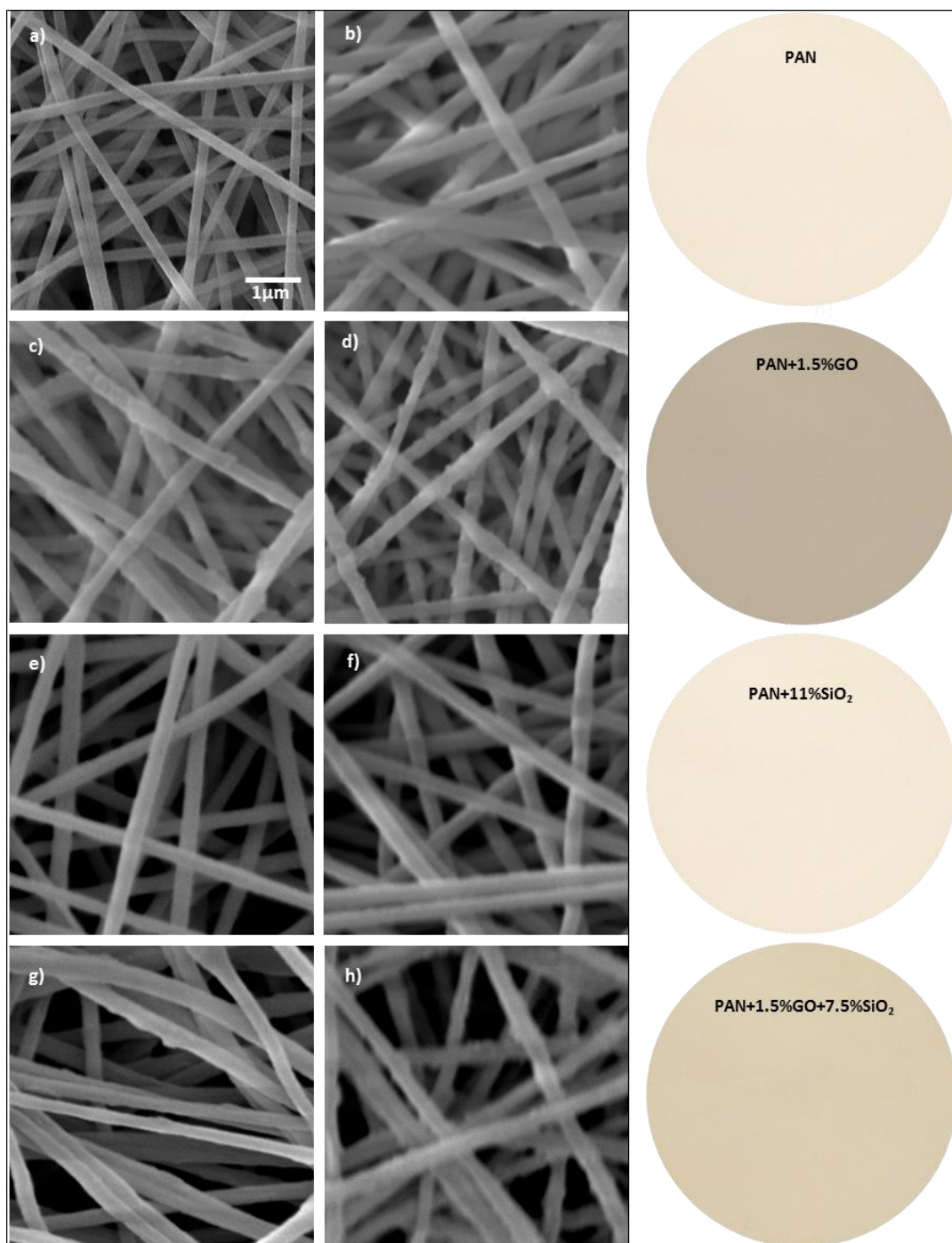


Figure 21.(left) SEM images of PAN based membranes, a) PAN, b) PAN-4SiO₂, c) PAN-7.5SiO₂, d) PAN-11SiO₂, e) PAN-0.5GO, f) PAN-1.5GO, g) PAN-4GO, h) PAN-1.5GO-7.5SiO₂, (right) Digital images of the electrospun membranes

This 3D microporous structure could facilitate high liquid permeation due to low resistance to mass transfer. The surface morphology changed with the addition of submicron particles of graphene oxide and silica. At low concentrations of silica, most of the particles are embedded within the fibers of polyacrylonitrile. As the concentration of silica increases, there are more chances of silica to come out at the fibrous surface which is confirmed by SEM images, thus creating a more roughened surface. It can also be noted that the average fiber diameter at highest silica concentration is decreased from 300nm to 285nm when compared to the lowest silica content of 4% SiO₂. This reduction in diameter is probably due to the reduction in conductivity and viscosity of the solution. Low solution viscosity favors the generation of thinner fibers. The formation of multi-level protrusions with increased SiO₂ content could be attributed to varying degrees of evaporation of the solution jet followed by rapid phase separation during the electrospinning process [113][114]. Graphene oxide additions created fibers with a thicker diameter which could be because of the increased viscosity due to graphene oxide. This increased viscosity of the electrospinning dope solution reduced the stretching of fibers during electrospinning that caused thicker fibers [115]. We have also noticed that the most of graphene oxide is embedded within the PAN fibers confirming high compatibility between the polymer and the filler. The emergence of swelled fibers or knotted structure with GO addition could be because of the size mismatch between the sub-micron GO sheets and the polymer fibers [88]. The high interaction between PAN and GO causes the PAN molecules to adhere onto the large GO sheets and swelled fibers or ellipsoids are formed [116]. In the case of hybrid fibers composed of PAN, GO and SiO₂, it is observed similar morphology. The combination of nanoscale silica and micro-nano graphene oxide caused the appearance of

nano-protrusions and the swelled fibers at some localized locations. As discussed above, these nano protrusions are because of the varying evaporation rates of the solvent while the appearance of the swelled fibers could be because of the size mismatch between the GO sheets and the polymer fibers. The high magnification images of the silica powder (figure 22 a-b) confirmed that the size of silica is between 10-20 nm.

We have also conducted transmission electron microscopy (TEM) (figure 22 c-d) to see the morphology of individual fibers of the hybrid membrane. It seems that the brightness of the swelled region is non-uniform compared to the smooth regions of the fiber. This appearance of dark and bright regions at the swelled/spindle knotted region confirms the existence of GO sheets as skeleton within the fibrous network which comes because of the difference in electron density [117]. We have also noticed nano level dark spots, which could be silica particles come out at the surface due to the reason explained earlier this section. Highly magnified TEM images also revealed the obvious agglomeration of nano-additives. The reason for the agglomeration could be the rapid evaporation of the DMF during electrospinning. Thus, these observations are consistent with the SEM analysis.

As discussed earlier, the surface chemical composition of the membrane is very important for effective separation. An electrospun membrane for separating dispersed oil in water phase should have the required functionalities to be able to satisfy its function. The FTIR spectra for PAN with varying concentrations of silica (SiO_2) (4% and 11%), graphene oxide (GO) (1.5% and 4%) and with fixed concentrations of silica (7.5%) and graphene oxide (1.5%) in hybrid (PAN-GO- SiO_2) membrane is shown (figure 23a).

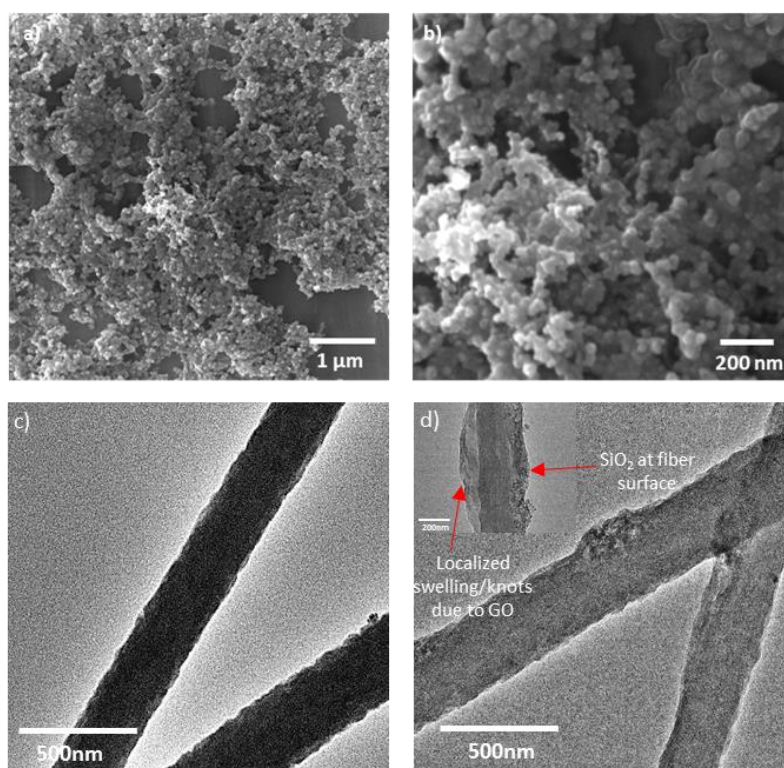
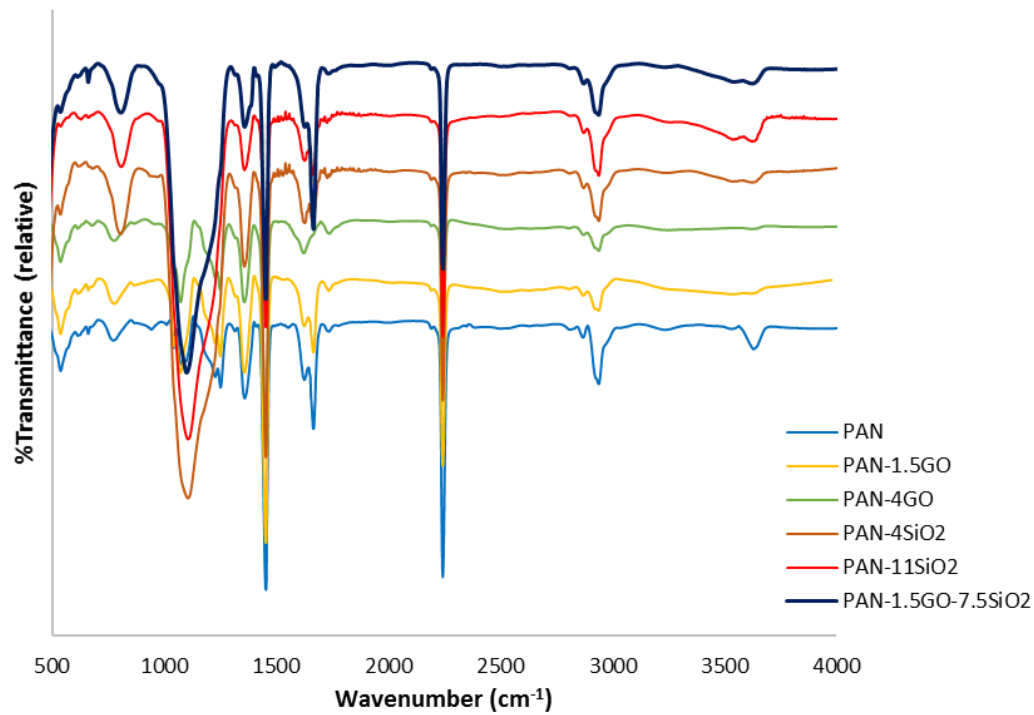


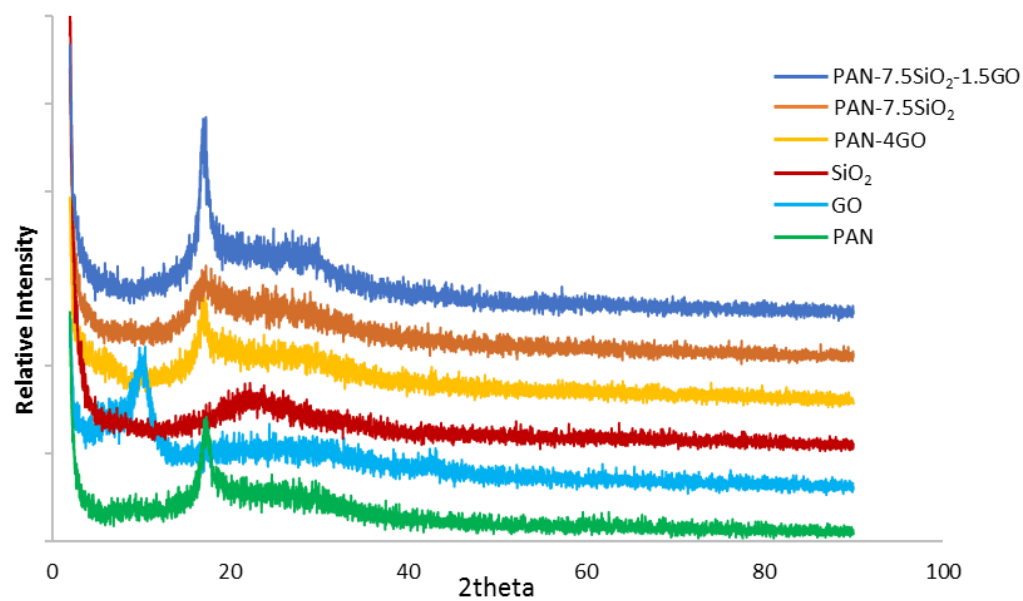
Figure 22. SEM images of SiO₂ nano powder (a-b), TEM images of electrospun pristine PAN and PAN-1.5GO-7.5SiO₂ membrane (c-d)

All the spectra show a characteristic peak of nitrile group at 2242cm^{-1} of PAN. While peaks from 2800-2950 correspond to C-H and $-\text{CH}_2-$ vibrations. The new peak appeared in PAN-SiO₂ composite membranes near 1100 cm^{-1} corresponds to Si-O-Si stretching vibration while the broad band appeared near 3390 cm^{-1} can be assigned to O-H vibrations of silica [118], [119]. These peaks are intensified with increased concentrations of silica. When comparing the spectra of PAN-GO with that of pristine PAN, it is observed that no new characteristic peaks appear with the addition of GO. Although the existence of GO could be confirmed by a small increase in peak intensity at 1731 cm^{-1} corresponds to C=O vibration of GO [109]. The reason for non-appearance of new peaks could be either that there was no change in chemical structure of polyacrylonitrile due to the addition of graphene oxide or GO might create bonds within the polymer chains [116].

PAN-based membranes were also analyzed through XRD technique to verify the chemical nature (figure 23b). For comparison, we had also taken the XRD patterns of GO and SiO₂ powder. XRD pattern of GO and SiO₂ powder, pristine PAN and hybrid PAN-based membranes with varying percentages of silica and graphene oxide. In the XRD pattern of pristine PAN, the sharp peak near 17° and a smaller broader region is observed. The peak at 17 degrees corresponds to 100 plane representing crystalline nature of PAN while the small broader peak which is usually reported for PAN indicates amorphous region [120]. The same peaks at 17° (2θ) also found in XRD patterns of PAN-GO, PAN-SiO₂ and PAN-GO-SiO₂ hybrid membranes representing a good interaction between inorganic fillers and the polymer.



a) FTIR spectra of PAN-Composite membranes



b) XRD Patterns of PAN-Composite membranes

Figure 23. FTIR spectra (a) and XRD pattern(b) of PAN-composite electrospun membranes

Strong reflection is observed in XRD pattern of PAN-GO-SiO₂ membrane, which could be because of the increased crystallinity of hybrid membrane due to the addition of small amount of GO.

Although the pattern of PAN-GO membrane did not show this increase in intensity which could be because GO in small amount behaves as crystal nuclei while at higher amounts can confine the polymer chains crystallization [116]. It was reported in the previous studies that the addition of silica of nanometer-sized range can decrease the crystalline region effectively [121]. During XRD analysis of PAN-SiO₂ electrospun membrane, we found that the intensity of the characteristic peak of PAN at 17° (2θ) angle decreases. The decrease in intensity reflects that dispersion of silica is uniform and it promotes the amorphous phase in the membrane [120].

Pore size and porosity of a membrane are very important properties. A membrane should have a pore size that can effectively block the desired component while creating minimum resistance to the flow of rest of the component. Pore size data of pristine PAN, PAN-SiO₂, PAN-GO and PAN-SiO₂-GO hybrid electrospun membranes (figure 24) revealed that all the membranes have similar pore sizes of 1-1.4 μm. The addition of inorganic fillers such as silica and graphene oxide have not really change the pore size. Thus, these membranes are expected to treat the emulsions which have droplet sizes of 1μm or higher which is usually the case for oil in water emulsions.

The high rate of separation requires the membranes to be highly porous. Electrospinning has proved itself to be a method of producing highly porous membranes [86]. Porosity measurements had carried out to determine the separation behavior PAN based

membranes. As mentioned in table 6, the electrospun PAN-based membranes have the average porosity of 85%. The highest porosity of 88% is obtained for the hybrid membrane composed of PAN with small additions of GO and SiO₂.

Table 6. Surface characteristics of PAN/PAN-based membrane

Membrane	Fiber diameter (nm)	Porosity (%)	Water contact angle (°)	Oil contact angle (°)
PAN	200	85	15	125
PAN-4SiO ₂	300	87	12	145
PAN-7.5SiO ₂	286	85	10	150
PAN-11SiO ₂	284	88	20	160
PAN-0.5GO	326	85	20	143
PAN-1.5GO	285	86	9	160
PAN-4GO	292	88	10	150
PAN-7.5SiO ₂ - 1.5GO	355	88	13	150

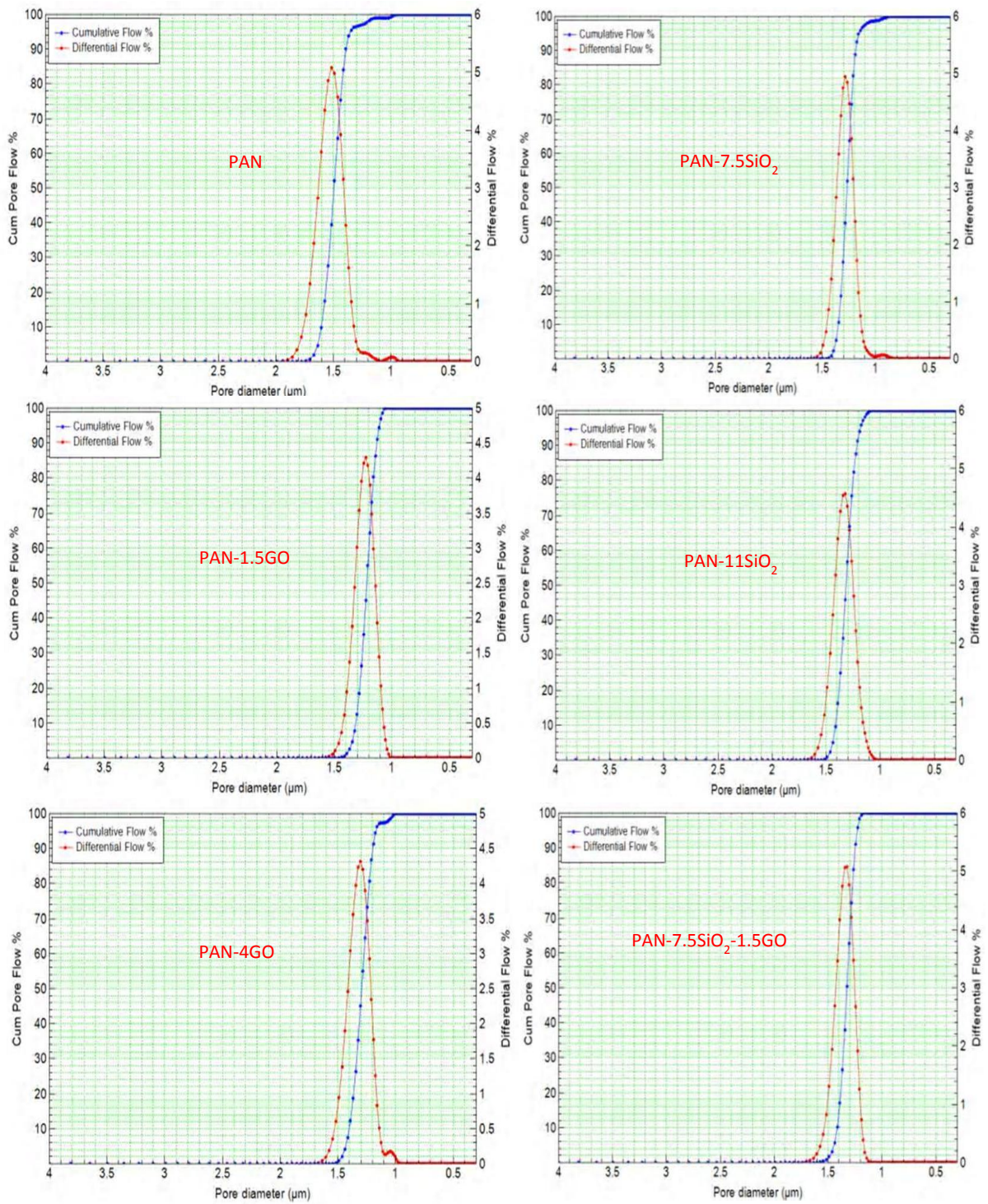


Figure 24. Showing pore size of electrospun PAN/PAN based membranes

These high values of porosity with interconnected 3D structure is supposed to have better separation characteristics such as high permeability at low pressure.

Mechanical properties are an important material aspect for any means of practical application. A membrane should have the required strength to work effectively in separation applications. Table 7 highlights the tensile behavior of the electrospun pan based membranes composed of inorganic fillers such as silica and graphene oxide. The initial tensile strength of pristine PAN membrane was 6.4 MPa. When the SiO₂ was added to make the PAN-SiO₂ composite membrane, the strength reduced. The strength of the composite goes down to 4.9 MPa with 4% SiO₂ with a further reduction at higher SiO₂ percentage while the ductility increased with adding silica. Although the purpose of adding nanofillers is often to reinforce the original matrix, here the strength decreased. It could be because of the disturbance in polymer chain interaction due to non-uniform distribution of silica particles [119]. When the graphene oxide was added into the polyacrylonitrile, the strength increases from 6.4 MPa to 9.1 MPa at 0.5% GO loading which could be because GO at low concentrations limits the chain misorientations of the polymer, thus improves the strength [122], [123]. Increasing the GO content further above 0.5% resulted in the reduction in tensile properties. The reason for this decrease could be same as discussed earlier in the case of SiO₂. Poor interfacial contact and agglomeration of GO sheets and silica particles on the nanofiber surface at higher concentrations may be responsible for the poor mechanical behavior of these membranes [124].

Table 7. Mechanical properties of PAN/PAN-based membranes

Membrane	Tensile strength (MPa)	Elongation (%)	Modulus (MPa)
PAN	6.4	17	118.1
PAN-11SiO₂	3.3	16.2	68.9
PAN-7.5SiO₂	4.6	25.1	76.7
PAN-4SiO₂	4.9	26	70.4
PAN-4GO	4.9	11	76.2
PAN-1.5GO	4.8	26.9	64.9
PAN-0.5GO	9.1	25.7	97.6
PAN-7.5SiO₂-1.5GO	7.4	13.9	128.1

Combination of superhydrophilicity (water attraction) and superoleophobicity (oil repulsion) is required for proper separation of oily water emulsions. Contact angles of water and underwater oil were investigated for the PAN-based composite-hybrid membranes to evaluate their wetting behavior (figure 25). Pristine PAN based electrospun membrane is inherently hydrophilic with a water contact angle of 15° and oil contact angle of 125° when the sample was placed under water. The water contact angle decreased and oil contact angle underwater increased when inorganic nanofillers are added. PAN-based membrane with smaller GO addition of 0.5%, showed higher oil contact angle of 143° and

similar water contact angle. When the content of GO further increased to 1.5%, the surface showed 160° underwater oil contact angle combined with a water contact angle of 9° . This increased in hydrophilicity confirmed that the introduction of GO improves water affinity of the membranes [88]. The reason of achieving high underwater contact angle for oil comes from a surface hierarchical structure composed of micro-nano features, which causes the water to sit inside the surface hierarchical features of individual fibers and forms a triple phase oil-water-solid condition.

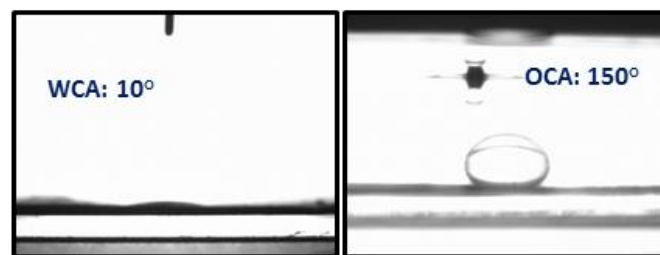
This water reduces the contact area of oil and causes the oil to be rolled off from the surface [110]. Addition of silica alone and in combination with graphene oxide also showed improved hydrophilic-oleophobic characteristics, which is because of the additional hydrophilic functionalities as confirmed by FTIR earlier. Due to this high hydrophilic and oleophobic characteristics, along with highly porous nature of the electrospinning process, PAN-based hybrid membranes are expected to behave efficiently for separating oil from a mixture of emulsified oily water.



(a) PAN only



(b) PAN-1.5GO



(c) PAN-7.5SiO₂



(d) PAN-7.5SiO₂-1.5GO

Figure 25. Water and underwater oil contact angles of PAN-composite membranes, (a) PAN, (b) PAN-1.5GO, (c) PAN-7.5SiO₂, (d) PAN-7.5SiO₂-1.5GO

4.6 Separation testing of PAN/PAN-based nanocomposite membranes

Due to high hydrophilicity together with surface hierarchy, our membranes showed a good combination of flux and efficiency. A series of PAN-based membranes consist of the pristine pan, composite PAN-GO, composite PAN-SiO₂ and hybrid PAN-GO-SiO₂ electrospun membranes were tested by fixing them on a dead-end filtration cell and an emulsion of oil in water was passed through it under a pressure of 0.1bar (height of liquid column without any external pressure) [88]. Digital and optical microscopic images of feed emulsions and permeates are presented (figure 26). The initial feed which was milky, turned to transparent after passing through our membranes, showed high separation efficiency. From the permeate flux data (figure 27) it is cleared that the incorporation of nanofillers improves the separation performance. The initial flux of 2600 L.m⁻².h⁻¹ for pristine PAN was increased to 3100 L.m⁻².h⁻¹ when GO and SiO₂ were added. This increase in flux is because of the increase in hydrophilicity which is already proved by the higher water contact angle. Repeated cycles of separation testing (figure 27 b) for PAN-hybrid membrane revealed that these membranes are effective for multiple usage. Here the silica specifically improved the water affinity of the inherently hydrophilic PAN while the purpose of adding GO was to enhance the effect of adding silica with the added antifouling characteristics. This antifouling behavior of graphene oxide can be revealed from the flux recovery in repeated cycles of oil-water separation test. It was also reported in the previous study of Zhang et al. [88], that the spindle-knots formed with the incorporation of GO, causes a better fouling resistance.

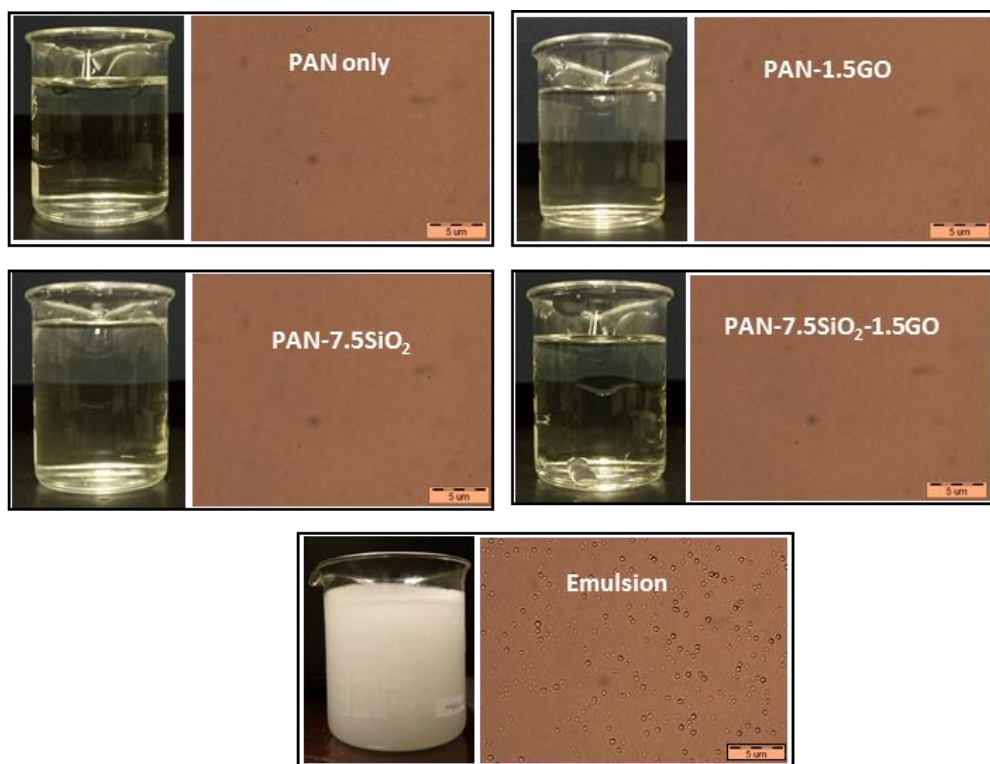
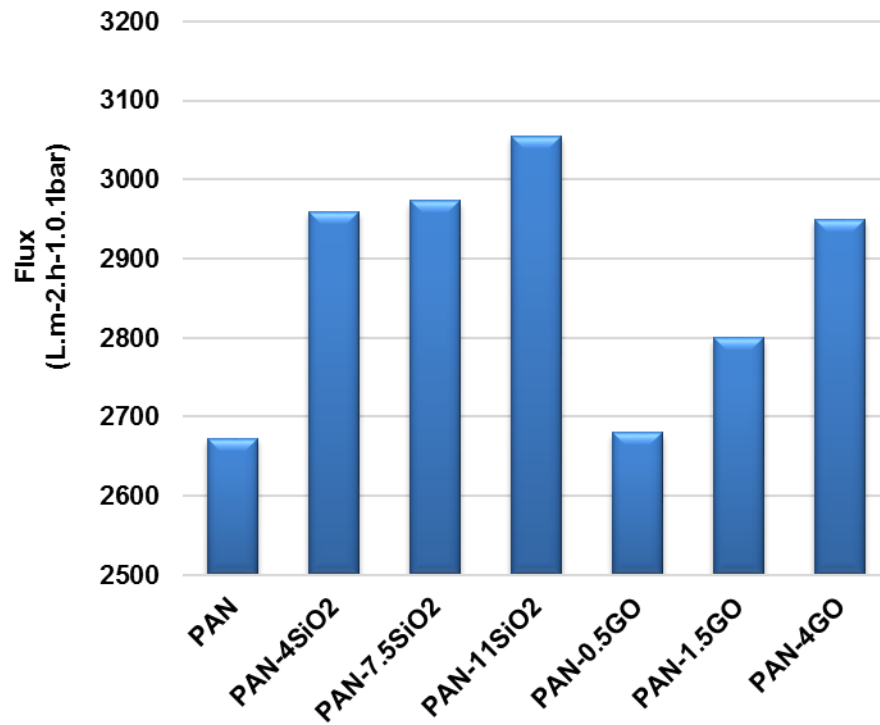
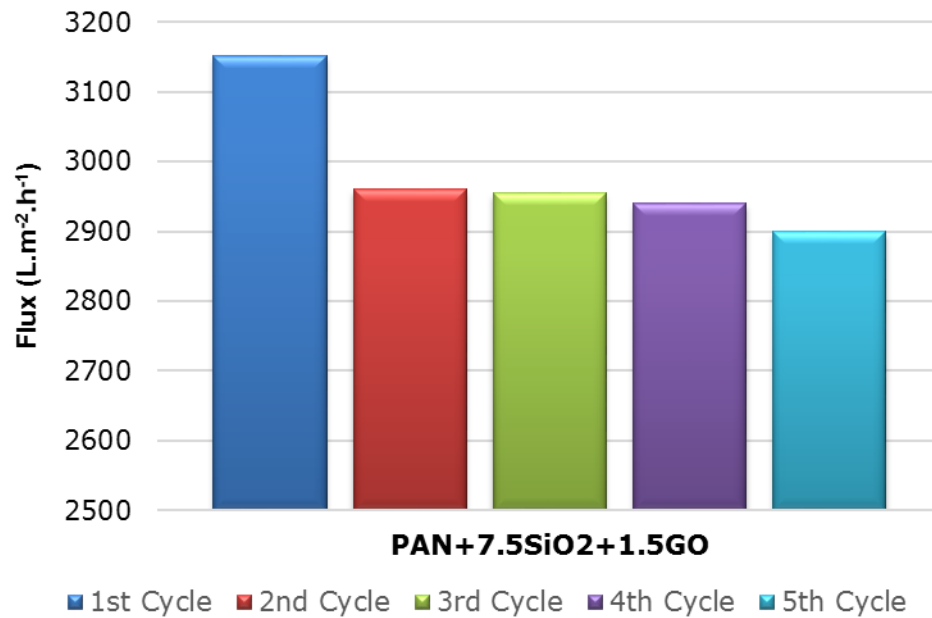


Figure 26. Separation performance of PAN-nano composite/hybrid electrospun membranes



a) Permeate flux of PAN-composite membranes

Flux vs Reusability



b) Permeate flux of PAN-hybrid membrane

Figure 27. Separation Flux of (a) PAN-Nanocomposite, and (b) hybrid membrane.

Quantitative analysis of the of the feed and permeates were carried out using organic carbon analyzer and efficiency of separation was calculated based on the organic carbon content of the permeate and feed emulsions. It was found that (table 8) the PAN-based membranes have 98% or higher rejection percentages for oil in water emulsion, thus are expected to be useful for real applications.

Table 8. Rejection (%) and flux of PAN-based membranes after oil-water separation

Sample	Rejection (%)	Flux (L.m⁻².h⁻¹)
PAN	98.8	2673
PAN-4SiO ₂	99.27	2960
PAN-7.5SiO ₂	99.25	2973
PAN-11SiO ₂	99.03	3055
PAN-0.5GO	98.97	2680
PAN-1.5GO	99.08	2800
PAN-4GO	98.94	2950
PAN-7.5SiO ₂ -1.5GO	99.27	3151

It can be observed that the PAN-based composite-hybrid membranes are useful for separating oil in water emulsions. Pure polyacrylonitrile membrane with highly porous entangled structure showed a separation efficiency of 98% while adding hydrophilic silica and antifouling graphene oxide, further enhanced the rejection percentage of oil to 99%.

4.7 Comparative analysis

We used different approaches here for the PAN based electrospun membranes for separating oil in water emulsions. Different characterizing tools were used to evaluate their behavior while separation of oil water emulsion is carried out for the performance evaluation. It was observed that all the approaches were successful in separating an oil in water emulsion with oil droplet sizes of 1-20 μ except the electrospun PAN membranes which were exposed to the vapors of solvent. Although the exposure to solvent vapors causes the membrane to densify and lowers its pore size but at the same time instead of improving the separation performance, resulted in significant decline in oil rejection percentage. Thus, it become unusable for the application of oil-water separation. The electrospun membrane which was treated with NaOH for 3-hour, showed separation performance with similar rejection % and permeate flux as that of hybrid membranes composed of PAN with 1.5%GO and 7.5%SiO₂. The mechanical properties and stability of these NaOH treated membranes should be same as that of untreated PAN membrane lower than the hybrid membrane. Coating PAN membranes with hydrogel-GO also showed good rejection but at lower flux than the hybrid membranes. Also coating made the process a two-step compared to one step process for hybrid membranes. Thus, the most feasible among all the membranes studied here, could be the hybrid PAN-GO-SiO₂ electrospun membrane considering good separation and mechanical properties. We observed that the hybrid membrane is also easy to clean simply by alternative water and ethanol rinsing and can be used repeatedly multiple times compared to the commercial PAN membrane (0.2 μ pore size, Sterlitech, USA), that after single time use became too brittle to be usable.

Table 9. Comparison of developed hybrid electrospun membrane with similar work

Materials	Method	Wetting behavior	Flux L.m⁻².h⁻¹	Tensile Strength (MPa)
SiO ₂ /Carbon [47]	Electrospinning + interfacial polymerization + carbonization	oleophilic	100	-
PIM-1/POSS [48]	Electrospinning	oleophilic	1097	-
HPAN/GO [88]	Electrospinning & Hydrolyzation	oleophobic	3500	-
PAN/SiO ₂ [95]	Electrospinning	oleophilic	3596	-
HPAN [23]	Casting	oleophobic	227	-
PAN-GO-SiO ₂ [present work]	Electrospinning	Oleophobic	3151	7.4

As shown in table 9, the hybrid membrane developed in this study is compared with the similar work. It can be noticed that only HPAN/GO and PAN/SiO₂ have better permeate flux than our membrane. PAN/SiO₂ membrane is oil wetting, thus for emulsions containing oils of lower density than water, which is usually the case for common oils, will not be effective as the oil will naturally goes upward and prevents the full separation. For HPAN/GO membrane, a water permeates flux of 3500 L.m⁻².h⁻¹ is reported which is still higher than our membrane, but the two-step process for the fabrication (electrospinning + hydrolyzation) makes this approach comparatively difficult if compared to the single step electrospinning process we used for the hybrid membrane.

CHAPTER 5

CONCLUSIONS AND RECOMMENDATIONS

5.1 Conclusions

Polyacrylonitrile (PAN)-based porous membrane for separating oil in water emulsion is developed using electrospinning process. Process parameters have a profound influence on the resultant fibrous morphology. Increasing the voltage causes the fibers to be rougher and smaller in diameter, however, increasing beyond a threshold value results in instability in the electrospinning process. For PAN-based membranes, the suitable voltage is found to be 20kV, yielding a good fibrous morphology. The flow rate of the polymer solution also causes an impact on the resultant mat. An increase in flow rate causes more volume of feed solution to come out from the needle tip, resulting in larger fibers, while reduced flow rate, below a threshold value, causes intermittent stops. These frequent stops, or more specifically disturbance, during fiber formation results in beaded fibrous morphology. These beads are considered as defects in the continuous fibrous network and can affect the separation performance. The flow rate of 1.0 ml/h is found to be suitable to produce small fiber diameter with reduced beads. The spinneret and collector speeds induce a change in the fibrous network. An increased speed results in more stretching during fiber collection and reduces the fiber diameter. But a high speed causes the fiber formation to be in un-stabilized condition and results in disturbed fibrous morphology. The values of 300 rpm and 70 mm/sec for the collector and spinneret speeds yield a stabilized fibrous morphology and small fiber diameter. Concentration of polymer solution is varied to obtain small fiber

diameter with a small pore size of the membrane mat. A range of 7-12 wt% PAN is electrospun, keeping the other process parameters constant. It is found that a low concentration gives finer fibers diameter, which increases with increasing the concentration. At 7% PAN, a lot of beads were found, thus 8% was selected as a suitable concentration yielding fine fibers and small pore size. Spinneret needle is also varied, the best needle diameter is 21G (0.6mm) as giving fine fibers with smooth morphology compared with 18G (0.8mm) which gives coarser fibers.

Inorganic nano-fillers are added to PAN-membrane to fabricate nanocomposite and hybrid electrospun membranes for oil-water emulsion separation. It is found that the incorporation of silica causes the development of micro-nano protrusions on the fibrous surface that become more prominent at higher silica concentration. The formation of multilevel protrusions could be attributed to varying degrees of evaporation of the solution jet followed by rapid phase separation during electrospinning. On the other hand, the incorporation of graphene oxide results in the formation of knots within the smooth fibrous network of PAN. The formation of these knots is believed to be caused by GO flakes, which might be oriented perpendicular to long dimension of the continuous fibers. Adding GO or SiO₂ alone, or in combination to develop a hybrid membrane, causes a significant increase in the separation performance while there is no measurable change found in the pore size, as it remains similar to that of pristine PAN membrane. The flux has increased to 3100 L.m⁻².h⁻¹ for hybrid membrane from the initial 2600 L.m⁻².h⁻¹ for pristine membrane due to enhanced hydrophilicity and surface hierarchical structure. The strength of electrospun membranes is also improved by incorporating nanofillers and reaches 9.1 MPa at 0.5% GO from initial 6.4 MPa for pristine PAN membrane. Further increase in GO or SiO₂

concentration is detrimental to mechanical properties (reduction in tensile strength) due to nonuniform distribution throughout the PAN fibrous structure.

Surface treatment of PAN-based membranes can also change the fibrous morphology and improve the performance. Hydrolysis of PAN membrane by NaOH results in the partial conversion of nitrile groups on PAN to the more hydrophilic carboxylic acid group. This increased hydrophilicity improves the separation performance of oil in water emulsion and yields a flux of more than $3100 \text{ L.m}^{-2}.\text{h}^{-1}$ for the PAN membrane hydrolyzed for 3 hours in 3M NaOH solution. Direct coating of PVA-GO through immersion for defined periods, also improves the hydrophilic characteristics due to the formation of hydrogen bonding between the constituents and inherent hydrophilic-antifouling properties of graphene oxide.

Exposing electrospun PAN membrane to the vapor of dimethylformamide (DMF) causes a significant reduction in pore size, due to fusion and merging of individual fibers. Despite this major reduction in pore size, it is found that the separation performance for oil in water emulsion is poor. This poor performance might be due to the destruction of the hierarchical structure of the fibrous network. However, this aspect needs further work to gain a better understanding of the underlying phenomena and come up with a proper conclusion.

5.2 Recommendations

Based on the above in-depth study towards the fabrication of efficient membranes for oil-water separation by electrospinning process, the following recommendations are made for future work.

- A separate study for surface treatment of electrospun PAN membrane should be conducted to further enhance the separation performance.
- Hydrogels should be directly electrospun together with nanofillers and crosslinked for better structural stability in water environment.
- Coaxial electrospinning should also be evaluated by selecting two different materials to prepare a membrane possessing a hydrophilic surface and a strong core.

References

- [1] J. A. Puangrat Kajitvichyanukul, Nazih K. Shamma, Yung-Tse Hung, Lawrence K. Wang, *Membrane and Desalination Technologies*, 2011th ed. The Humana Press Inc ., New York.
- [2] A. A. Al-Shamrani, A. James, and H. Xiao, “Destabilisation of oil-water emulsions and separation by dissolved air flotation,” *Water Res.*, vol. 36, no. 6, pp. 1503–1512, 2002.
- [3] J. Rubio, M. L. Souza, and R. W. Smith, “Overview of flotation as a wastewater treatment technique,” *Miner. Eng.*, vol. 15, no. 3, pp. 139–155, 2002.
- [4] M. Cheryan and N. Rajagopalan, “Membrane processing of oily streams. Wastewater treatment and waste reduction,” *J. Memb. Sci.*, vol. 151, no. 1, pp. 13–28, 1998.
- [5] G. G.-C. José Coca-Prados, *Water Purification and Management*, 2011th ed. Springer Netherlands, 2011.
- [6] Z. Chu, Y. Feng, and S. Seeger, “Oil/water separation with selective superantiwetting/superwetting surface materials,” *Angew. Chemie - Int. Ed.*, vol. 54, no. 8, pp. 2328–2338, 2015.
- [7] X. Zhu, H. E. Loo, and R. Bai, “A novel membrane showing both hydrophilic and oleophobic surface properties and its non-fouling performances for potential water treatment applications,” *J. Memb. Sci.*, vol. 436, pp. 47–56, 2013.
- [8] S. Wang *et al.*, “Advances in high permeability polymer-based membrane materials for CO₂ separations,” *Energy Environ. Sci.*, vol. 9, no. 6, pp. 1863–1890, 2016.
- [9] W. Cui, Y. Zhou, and J. Chang, “Electrospun nanofibrous materials for tissue engineering and drug delivery,” *Sci. Technol. Adv. Mater.*, vol. 11, no. 1, p. 14108, 2010.
- [10] S. Farhadi, M. Farzaneh, and S. A. Kulinich, “Anti-icing performance of superhydrophobic surfaces,” *Appl. Surf. Sci.*, vol. 257, no. 14, pp. 6264–6269, 2011.
- [11] S. Lee and W. Rahwang, “Large-area superhydrophobic nanofiber array structures for drag reduction,” *17th Int. Conf.*, 2009.
- [12] B. S. Lalia, E. Guillen, H. A. Arafat, and R. Hashaikeh, “Nanocrystalline cellulose reinforced PVDF-HFP membranes for membrane distillation application,” *Desalination*, vol. 332, no. 1, pp. 134–141, 2014.
- [13] W. Barthlott and C. Neinhuis, “Purity of the sacred lotus, or escape from

- contamination in biological surfaces,” *Planta*, vol. 202, no. 1, pp. 1–8, 1997.
- [14] P. R. Waghmare, N. S. K. Gunda, and S. K. Mitra, “Under-water superoleophobicity of fish scales,” *Sci. Rep.*, vol. 4, p. 7454, 2014.
- [15] M. Liu, S. Wang, Z. Wei, Y. Song, and L. Jiang, “Bioinspired design of a superoleophobic and low adhesive water/solid interface,” *Adv. Mater.*, vol. 21, no. 6, pp. 665–669, 2009.
- [16] R. N. Wenzel, “Resistance of solid surfaces to wetting by water.,” *J. Ind. Eng. Chem. (Washington, D. C.)*, vol. 28, pp. 988–994, 1936.
- [17] K. Tsujii, T. Yamamoto, T. Onda, and S. Shibuichi, “Super Oil-Repellent Surfaces,” *Angew. Chemie Int. Ed. English*, vol. 36, pp. 1011–1012, 1997.
- [18] S. Shibuichi, T. Yamamoto, T. Onda, and K. Tsujii, “Super Water- and Oil-Repellent Surfaces Resulting from Fractal Structure,” *J. Colloid Interface Sci.*, vol. 208, no. 1, pp. 287–294, 1998.
- [19] A. Tuteja, W. Choi, J. M. Mabry, G. H. McKinley, and R. E. Cohen, “Robust omniphobic surfaces.,” *Proc. Natl. Acad. Sci. U. S. A.*, vol. 105, pp. 18200–18205, 2008.
- [20] A. K. Holda and I. F. J. Vankelecom, “Understanding and guiding the phase inversion process for synthesis of solvent resistant nanofiltration membranes,” *J. Appl. Polym. Sci.*, vol. 132, no. 27, pp. 1–17, 2015.
- [21] W. Zhang, Z. Shi, F. Zhang, X. Liu, J. Jin, and L. Jiang, “Superhydrophobic and superoleophilic PVDF membranes for effective separation of water-in-oil emulsions with high flux,” *Adv. Mater.*, vol. 25, no. 14, pp. 2071–2076, 2013.
- [22] W. Zhang *et al.*, “Salt-induced fabrication of superhydrophilic and underwater superoleophobic PAA-g-PVDF membranes for effective separation of oil-in-water emulsions,” *Angew. Chemie - Int. Ed.*, vol. 53, no. 3, pp. 856–860, 2014.
- [23] F. Zhang, S. Gao, Y. Zhu, and J. Jin, “Alkaline-induced superhydrophilic/underwater superoleophobic polyacrylonitrile membranes with ultralow oil-adhesion for high-efficient oil/water separation,” *J. Memb. Sci.*, vol. 513, pp. 67–73, 2016.
- [24] M. a. Masuelli, “Ultrafiltration of oil/water emulsions using PVDF/PC blend membranes,” *Desalin. Water Treat.*, vol. 53, no. 3, pp. 569–578, 2015.
- [25] N. A. Ochoa, M. Masuelli, and J. Marchese, “Effect of hydrophilicity on fouling of an emulsified oil wastewater with PVDF/PMMA membranes,” *J. Memb. Sci.*, vol. 226, no. 1–2, pp. 203–211, 2003.
- [26] K. Matyjaszewski, “Atom Transfer Radical Polymerization and the Synthesis of Polymeric Materials,” *Adv. Mater.*, vol. 10, no. 12, pp. 901–915, 1998.

- [27] B. Chakrabarty, A. K. Ghoshal, and M. K. Purkait, "Cross-flow ultrafiltration of stable oil-in-water emulsion using polysulfone membranes," *Chem. Eng. J.*, vol. 165, no. 2, pp. 447–456, 2010.
- [28] B. Chakrabarty, A. K. Ghoshal, and M. K. Purkait, "Ultrafiltration of stable oil-in-water emulsion by polysulfone membrane," *J. Memb. Sci.*, vol. 325, no. 1, pp. 427–437, 2008.
- [29] H. Strathmann and K. Kock, "The formation mechanism of phase inversion membranes," *Desalination*, vol. 21, no. 3, pp. 241–255, 1977.
- [30] A. Kausar, "Phase Inversion Technique-Based Polyamide Films and Their Applications: A Comprehensive Review," *Polym. Plast. Technol. Eng.*, p. 03602559.2016.1276593, Jan. 2017.
- [31] P. S. Brown and B. Bhushan, "Mechanically durable, superoleophobic coatings prepared by layer-by-layer technique for anti-smudge and oil-water separation," *Sci. Rep.*, vol. 5, p. 8701, 2015.
- [32] M. E. Buck, S. C. Schwartz, and D. M. Lynn, "Superhydrophobic Thin Films Fabricated by Reactive Layer-by-Layer Assembly of Azlactone-Functionalized Polymers," *Chem. Mater.*, vol. 22, no. 23, pp. 6319–6327, Dec. 2010.
- [33] L. Zhai, F. C. Cebeci, R. E. Cohen, and M. F. Rubner, "Stable superhydrophobic coatings from polyelectrolyte multilayers," *Nano Lett.*, vol. 4, no. 7, pp. 1349–1353, 2004.
- [34] X. Lin, M. Yang, H. Jeong, M. Chang, and J. Hong, "Durable superhydrophilic coatings formed for anti-biofouling and oil-water separation," *J. Memb. Sci.*, vol. 506, pp. 22–30, 2016.
- [35] M. Liu, J. Li, and Z. Guo, "Polyaniline coated membranes for effective separation of oil-in-water emulsions," *J. Colloid Interface Sci.*, vol. 467, pp. 261–270, 2016.
- [36] R. Ou, J. Wei, L. Jiang, G. P. Simon, and H. Wang, "Robust Thermoresponsive Polymer Composite Membrane with Switchable Superhydrophilicity and Superhydrophobicity for Efficient Oil-Water Separation," *Environ. Sci. Technol.*, vol. 50, no. 2, pp. 906–914, 2016.
- [37] H. Yoon *et al.*, "Gravity-Driven Hybrid Membrane for Oleophobic – Superhydrophilic Oil – Water Separation and Water Purification by Graphene," *Langmuir*, vol. 30, no. 39, pp. 11761–11769, 2014.
- [38] A. K. Kota, G. Kwon, W. Choi, J. M. Mabry, and A. Tuteja, "Hygro-responsive membranes for effective oil-water separation," *Nat. Commun.*, vol. 3, p. 1025, 2012.
- [39] S. J. Gao, Z. Shi, W. Bin Zhang, F. Zhang, and J. Jin, "Photoinduced superwetting single-walled carbon nanotube/TiO₂ ultrathin network films for ultrafast separation of oil-in-water emulsions," *ACS Nano*, vol. 8, no. 6, pp. 6344–6352,

2014.

- [40] Z. Shi *et al.*, “Ultrafast separation of emulsified oil/water mixtures by ultrathin free-standing single-walled carbon nanotube network films,” *Adv. Mater.*, vol. 25, no. 17, pp. 2422–2427, 2013.
- [41] L. Hu, S. J. Gao, Y. Z. Zhu, F. Zhang, L. Jiang, and J. Jin, “An ultrathin bilayer membrane with asymmetric wettability for pressure responsive oil/water emulsion separation,” *J. Mater. Chem. A*, vol. 3, no. 46, pp. 23477–23482, 2015.
- [42] C. Te Hsieh, J. P. Hsu, H. H. Hsu, W. H. Lin, and R. S. Juang, “Hierarchical oil-water separation membrane using carbon fabrics decorated with carbon nanotubes,” *Surf. Coatings Technol.*, vol. 286, pp. 148–154, 2016.
- [43] P. Chen and Z. Xu, “Mineral-coated polymer membranes with superhydrophilicity and underwater superoleophobicity for effective oil/water separation,” *Sci. Rep.*, vol. 3, p. 2776, 2013.
- [44] M. Obaid, N. A. M. Barakat, O. A. Fadali, M. Motlak, A. A. Almajid, and K. A. Khalil, “Effective and reusable oil/water separation membranes based on modified polysulfone electrospun nanofiber mats,” *Chem. Eng. J.*, vol. 259, pp. 449–456, 2015.
- [45] F. Ejaz Ahmed, B. S. Lalia, N. Hilal, and R. Hashaikeh, “Underwater superoleophobic cellulose/electrospun PVDF-HFP membranes for efficient oil/water separation,” *Desalination*, vol. 344, pp. 48–54, 2014.
- [46] A. Raza, B. Ding, G. Zainab, M. El-Newehy, S. S. Al-Deyab, and J. Yu, “In situ cross-linked superwetting nanofibrous membranes for ultrafast oil–water separation,” *J. Mater. Chem. A*, vol. 2, pp. 10137–10145, 2014.
- [47] M. H. Tai, J. Juay, D. D. Sun, and J. O. Leckie, “Carbon-silica composite nanofiber membrane for high flux separation of water-in-oil emulsion - Performance study and fouling mechanism,” *Sep. Purif. Technol.*, vol. 156, pp. 952–960, 2015.
- [48] C. Zhang, P. Li, and B. Cao, “Electrospun Microfibrous Membranes Based on PIM-1/POSS with High Oil Wettability for Separation of Oil-Water Mixtures and Cleanup of Oil Soluble Contaminants,” *Ind. Eng. Chem. Res.*, vol. 54, no. 35, pp. 8772–8781, 2015.
- [49] Y. Long *et al.*, “Hydrogen bond nanoscale networks showing switchable transport performance,” *Sci. Rep.*, vol. 2, p. 612, 2012.
- [50] L. Chen, Y. Si, H. Zhu, T. Jiang, and Z. Guo, “A study on the fabrication of porous PVDF membranes by in-situ elimination and their applications in separating oil/water mixtures and nano-emulsions,” *J. Memb. Sci.*, vol. 520, pp. 760–768, 2016.
- [51] J. Liu, P. Li, L. Chen, Y. Feng, W. He, and X. Lv, “Modified superhydrophilic and

- underwater superoleophobic PVDF membrane with ultralow oil-adhesion for highly efficient oil/water emulsion separation,” *Mater. Lett.*, vol. 185, pp. 169–172, 2016.
- [52] H. Shi *et al.*, “A modified mussel-inspired method to fabricate TiO₂ decorated superhydrophilic PVDF membrane for oil/water separation,” *J. Memb. Sci.*, vol. 506, pp. 60–70, 2016.
- [53] K. Venkatesh, G. Arthanareeswaran, and A. C. Bose, “PVDF mixed matrix nanofiltration membranes integrated with 1D-PANI/TiO₂ NFs for oil-water emulsion separation,” *RSC Adv.*, vol. 6, no. 23, pp. 18899–18908, 2016.
- [54] W. Fang *et al.*, “Electrospun N-Substituted Polyurethane Membranes with Self-Healing Ability for Self-Cleaning and Oil/Water Separation,” *Chem. - A Eur. J.*, vol. 22, no. 3, pp. 878–883, 2016.
- [55] X. Lin, M. Yang, H. Jeong, M. Chang, and J. Hong, “Durable superhydrophilic coatings formed for anti-biofouling and oil – water separation,” *J. Memb. Sci.*, vol. 506, pp. 22–30, 2016.
- [56] L. Q. Ning, N. K. Xu, R. Wang, and Y. Liu, “Fibrous membranes electrospun from the suspension polymerization product of styrene and butyl acrylate for oil – water separation,” pp. 57101–57113, 2015.
- [57] R. Ou, J. Wei, L. Jiang, G. P. Simon, and H. Wang, “Robust Thermoresponsive Polymer Composite Membrane with Switchable Superhydrophilicity and Superhydrophobicity for Efficient Oil-Water Separation,” *Environ. Sci. Technol.*, vol. 50, no. 2, pp. 906–914, 2016.
- [58] G. G. Chase, S. Swaminathan, and B. Raghavan, “7 - Functional nanofibers for filtration applications A2 - Wei, Qufu BT - Functional Nanofibers and their Applications,” in *Woodhead Publishing Series in Textiles*, Woodhead Publishing, 2012, pp. 121–152.
- [59] N. Bhardwaj and S. C. Kundu, “Electrospinning: A fascinating fiber fabrication technique,” *Biotechnol. Adv.*, vol. 28, no. 3, pp. 325–347, 2010.
- [60] L. Li and Y. Lo Hsieh, “Ultra-fine polyelectrolyte fibers from electrospinning of poly(acrylic acid),” *Polymer (Guildf.)*, vol. 46, no. 14, pp. 5133–5139, 2005.
- [61] R. Baba, C. J. Angamma, S. H. Jayaram, and L. T. Lim, “Electrospinning of Alginate and Poly-ethylene Oxide Blends Using Pulsed Electric Fields to Fabricate Chopped Nanofibres,” *Proc. ESA Annu. Meet. Electrostat.*, pp. 1–8, 2010.
- [62] H. T. Zhu, S. S. Qiu, W. Jiang, D. X. Wu, and C. Y. Zhang, “Evaluation of Electrospun Polyvinyl Chloride/Polystyrene Fibers As Sorbent Materials for Oil Spill Cleanup,” *Environ. Sci. Technol.*, vol. 45, no. 10, pp. 4527–4531, 2011.
- [63] Z. L. Xu, B. Zhang, and J. K. Kim, “Electrospun carbon nanofiber anodes containing monodispersed Si nanoparticles and graphene oxide with exceptional

- high rate capacities,” *Nano Energy*, vol. 6, pp. 27–35, 2014.
- [64] H. Junoh *et al.*, “A Review on the Fabrication of Electrospun Polymer Electrolyte Membrane for Direct Methanol Fuel Cell,” *J. Nanomater.*, vol. 2015, pp. 1–16, 2014.
- [65] Y. Zhu, L. Feng, F. Xia, J. Zhai, M. Wan, and L. Jiang, “Chemical dual-responsive wettability of superhydrophobic PANI-PAN coaxial nanofibers,” *Macromol. Rapid Commun.*, vol. 28, no. 10, pp. 1135–1141, 2007.
- [66] M. Obaid *et al.*, “Effective polysulfone-amorphous SiO₂/NPs electrospun nanofiber membrane for high flux oil/water separation,” *Chem. Eng. J.*, vol. 279, pp. 631–638, 2015.
- [67] W. E. Teo and S. Ramakrishna, “A review on electrospinning design and nanofibre assemblies,” *Nanotechnology*, vol. 17, no. 14, pp. R89–R106, 2006.
- [68] R. Wang, Y. Liu, B. Li, B. S. Hsiao, and B. Chu, “Electrospun nanofibrous membranes for high flux microfiltration,” *J. Memb. Sci.*, vol. 392–393, pp. 167–174, 2012.
- [69] G. Eda and S. Shivkumar, “Bead-to-fiber transition in electrospun polystyrene,” *J. Appl. Polym. Sci.*, vol. 106, no. 1, pp. 475–487, Oct. 2007.
- [70] W. Cui, X. Li, S. Zhou, and J. Weng, “Investigation on process parameters of electrospinning system through orthogonal experimental design,” *J. Appl. Polym. Sci.*, vol. 103, no. 5, pp. 3105–3112, Mar. 2007.
- [71] S. Wongsasulak, K. M. Kit, D. J. McClements, T. Yoovidhya, and J. Weiss, “The effect of solution properties on the morphology of ultrafine electrospun egg albumen–PEO composite fibers,” *Polymer (Guildf.)*, vol. 48, no. 2, pp. 448–457, Jan. 2007.
- [72] E. Biber, G. Gündüz, B. Mavis, and U. Colak, “Effects of electrospinning process parameters on nanofibers obtained from Nylon 6 and poly (ethylene-n-butyl acrylate-maleic anhydride) elastomer blends using Johnson SB statistical distribution function,” *Appl. Phys. A Mater. Sci. Process.*, vol. 99, no. 2, pp. 477–487, 2010.
- [73] X. Yuan, Y. Zhang, C. Dong, and J. Sheng, “Morphology of ultrafine polysulfone fibers prepared by electrospinning,” *Polym. Int.*, vol. 53, no. 11, pp. 1704–1710, Nov. 2004.
- [74] C. Zhang, X. Yuan, L. Wu, Y. Han, and J. Sheng, “Study on morphology of electrospun poly(vinyl alcohol) mats,” *Eur. Polym. J.*, vol. 41, no. 3, pp. 423–432, Mar. 2005.
- [75] O. S. Yördem, M. Papila, and Y. Z. Menceloğlu, “Effects of electrospinning parameters on polyacrylonitrile nanofiber diameter: An investigation by response surface methodology,” *Mater. Des.*, vol. 29, no. 1, pp. 34–44, Jan. 2008.

- [76] C. J. Buchko, L. C. Chen, Y. Shen, and D. C. Martin, "Processing and microstructural characterization of porous biocompatible protein polymer thin films," *Polymer (Guildf)*, vol. 40, no. 26, pp. 7397–7407, Dec. 1999.
- [77] B. Ding, M. Wang, X. Wang, J. Yu, and G. Sun, "Electrospun nanomaterials for ultrasensitive sensors," *Mater. Today*, vol. 13, no. 11, pp. 16–27, Nov. 2010.
- [78] B.-M. Min, G. Lee, S. H. Kim, Y. S. Nam, T. S. Lee, and W. H. Park, "Electrospinning of silk fibroin nanofibers and its effect on the adhesion and spreading of normal human keratinocytes and fibroblasts in vitro," *Biomaterials*, vol. 25, no. 7–8, pp. 1289–1297, Mar. 2004.
- [79] X. Wang, J. Yu, G. Sun, and B. Ding, "Electrospun nanofibrous materials: A versatile medium for effective oil/water separation," *Mater. Today*, vol. 0, no. 0, pp. 0–11, 2016.
- [80] W. Ma *et al.*, "Electrospun fibers for oil-water separation," *RSC Adv.*, vol. 6, no. 16, pp. 12868–12884, 2016.
- [81] M. W. Lee, S. An, S. S. Lathe, C. Lee, S. Hong, and S. S. Yoon, "Electrospun polystyrene nanofiber membrane with superhydrophobicity and superoleophilicity for selective separation of water and low viscous oil," *ACS Appl. Mater. Interfaces*, vol. 5, no. 21, pp. 10597–10604, 2013.
- [82] M. H. Tai, P. Gao, B. Y. L. Tan, D. D. Sun, and J. O. Leckie, "Highly Efficient and Flexible Electrospun Carbon–Silica Nanofibrous Membrane for Ultrafast Gravity-Driven Oil–Water Separation," *ACS Appl. Mater. Interfaces*, vol. 6, no. 12, pp. 9393–9401, Jun. 2014.
- [83] V. A. Ganesh *et al.*, "Electrospun Differential Wetting Membranes for Efficient Oil-Water Separation," *Macromol. Mater. Eng.*, vol. 301, no. 7, pp. 812–817, Jul. 2016.
- [84] Y. Ning, L.Q.; Xu, N.K.; Wang, R.; Liu, "Fibrous membranes electrospun from the suspension polymerization product of styrene and butyl acrylate for oil-water separation," *RCS Adv.*, vol. 5, p. 57101, 2015.
- [85] H. Ma, C. Burger, B. S. Hsiao, and B. Chu, "Ultra-fine cellulose nanofibers: new nano-scale materials for water purification," *J. Mater. Chem.*, vol. 21, no. 21, pp. 7507–7510, 2011.
- [86] H. Che *et al.*, "CO₂-Responsive Nanofibrous Membranes with Switchable Oil / Water Wettability," *Angew. Chemie - Int. Ed.*, no. 2011cb 935700, pp. 1–6, 2015.
- [87] J. Zhang *et al.*, "Graphene oxide/polyacrylonitrile fiber hierarchical-structured membrane for ultra-fast microfiltration of oil-water emulsion," *Chem. Eng. J.*, vol. 307, pp. 643–649, 2017.
- [88] J. Zhang, X. Pan, Q. Xue, D. He, L. Zhu, and Q. Guo, "Antifouling hydrolyzed polyacrylonitrile/graphene oxide membrane with spindle-knotted structure for

- highly effective separation of oil-water emulsion,” *J. Memb. Sci.*, vol. 532, no. March, pp. 38–46, 2017.
- [89] M. Obaid, O. A. Fadali, B. Lim, H. Fouad, and N. A. M. Barakat, “Super-hydrophilic and highly stable in oils polyamide-polysulfone composite membrane by electrospinning,” *Mater. Lett.*, vol. 138, pp. 196–199, 2015.
- [90] P. Zhang, R. Tian, R. Lv, B. Na, and Q. Liu, “Water-permeable polylactide blend membranes for hydrophilicity-based separation,” *Chem. Eng. J.*, vol. 269, pp. 180–185, 2015.
- [91] S. Kaur, S. Sundarrajan, D. Rana, T. Matsuura, and S. Ramakrishna, “Influence of electrospun fiber size on the separation efficiency of thin film nanofiltration composite membrane,” *J. Memb. Sci.*, vol. 392–393, pp. 101–111, 2012.
- [92] X. Cao, M. Huang, B. Ding, J. Yu, and G. Sun, “Robust polyacrylonitrile nanofibrous membrane reinforced with jute cellulose nanowhiskers for water purification,” *Desalination*, vol. 316, pp. 120–126, 2013.
- [93] W. Panatdasirisuk, Z. Liao, T. Vongsetskul, and S. Yang, “Separation of Oil-in-Water Emulsions Using Hydrophilic Electrospun Membranes with Anisotropic Pores,” *Langmuir*, vol. 33, no. 23, pp. 5872–5878, Jun. 2017.
- [94] Y. Chen *et al.*, “Fabrication of Silica Nanospheres Coated Membranes : towards the Effective Separation of Oil-in-Water Emulsion in Extremely Acidic and Concentrated Salty Environments,” *Sci. Rep.*, vol. 6, no. August, pp. 1–8, 2016.
- [95] M. H. Tai, J. Juay, D. D. Sun, and J. O. Leckie, “Carbon-silica composite nanofiber membrane for high flux separation of water-in-oil emulsion - Performance study and fouling mechanism,” *Sep. Purif. Technol.*, vol. 156, pp. 952–960, 2015.
- [96] B. S. Lalia, E. Guillen-Burrieza, H. A. Arafat, and R. Hashaikeh, “Fabrication and characterization of polyvinylidene fluoride-co-hexafluoropropylene (PVDF-HFP) electrospun membranes for direct contact membrane distillation,” *J. Memb. Sci.*, vol. 428, pp. 104–115, 2013.
- [97] K. Yoon, B. S. Hsiao, and B. Chu, “High flux ultrafiltration nanofibrous membranes based on polyacrylonitrile electrospun scaffolds and crosslinked polyvinyl alcohol coating,” *J. Memb. Sci.*, vol. 338, no. 1–2, pp. 145–152, 2009.
- [98] K. Yoon, B. S. Hsiao, and B. Chu, “Formation of functional polyethersulfone electrospun membrane for water purification by mixed solvent and oxidation processes,” *Polymer (Guildf.)*, vol. 50, no. 13, pp. 2893–2899, 2009.
- [99] A. H. Hekmati, N. Khenoussi, H. Nouali, J. Patarin, and J.-Y. Drean, “Effect of nanofiber diameter on water absorption properties and pore size of polyamide-6 electrospun nanoweb,” *Text. Res. J.*, vol. 84, no. 19, pp. 2045–2055, 2014.
- [100] A. Rajak, “Synthesis of Electrospun Nanofibers Membrane and Its Optimization

- for Aerosol Filter Application,” *KnE Eng.*, vol. 1, no. 1, pp. 1–7, 2016.
- [101] S. Wong, “An Investigation of Process Parameters to Optimize the Fiber Diameter of Electrospun Vascular Scaffolds through Experimental Design,” 2010.
- [102] A. Manuscript, “NIH Public Access,” *Polymer (Guildf.)*, pp. 1–17, 2011.
- [103] J. Sutasinpromprae, S. Jitjaicham, M. Nithitanakul, C. Meechaisue, and P. Supaphol, “Preparation and characterization of ultrafine electrospun polyacrylonitrile fibers and their subsequent pyrolysis to carbon fibers,” *Polym. Int.*, vol. 55, no. 8, pp. 825–833, Aug. 2006.
- [104] V. Sencadas *et al.*, “Determination of the parameters affecting electrospun chitosan fiber size distribution and morphology,” *Carbohydr. Polym.*, vol. 87, no. 2, pp. 1295–1301, 2012.
- [105] T. H. Cheng, S. Y. Chou, Y. K. Chang, and H. C. Lee, “Fabrication of electrospun polyacrylonitrile ion-exchange membranes for protein purification,” *Taiwan Text. Res. J.*, vol. 23, no. 1, pp. 20–27, 2013.
- [106] S. Deng, R. Bai, and J. P. Chen, “Aminated polyacrylonitrile fibers for lead and copper removal,” *Langmuir*, vol. 19, no. 12, pp. 5058–5064, 2003.
- [107] S. Deng, R. Bai, and J. P. Chen, “Behaviors and mechanisms of copper adsorption on hydrolyzed polyacrylonitrile fibers,” *J. Colloid Interface Sci.*, vol. 260, no. 2, pp. 265–272, 2003.
- [108] Z. G. Wang, L. S. Wan, and Z. K. Xu, “Surface engineering of polyacrylonitrile-based asymmetric membranes towards biomedical applications: An overview,” *J. Memb. Sci.*, vol. 304, no. 1–2, pp. 8–23, 2007.
- [109] C. Cheng, L. Shen, X. Yu, Y. Yang, X. Li, and X. Wang, “Robust construction of a graphene oxide barrier layer on a nanofibrous substrate assisted by the flexible poly(vinylalcohol) for efficient pervaporation desalination,” *J. Mater. Chem. A*, vol. 5, no. 7, pp. 3558–3568, 2017.
- [110] Z. Xue *et al.*, “A novel superhydrophilic and underwater superoleophobic hydrogel-coated mesh for oil/water separation,” *Adv. Mater.*, vol. 23, no. 37, pp. 4270–4273, 2011.
- [111] J. B. Fan *et al.*, “Directly Coating Hydrogel on Filter Paper for Effective Oil-Water Separation in Highly Acidic, Alkaline, and Salty Environment,” *Adv. Funct. Mater.*, vol. 25, no. 33, pp. 5368–5375, 2015.
- [112] M. K. Leach, Z.-Q. Feng, S. J. Tuck, and J. M. Corey, “Electrospinning fundamentals: optimizing solution and apparatus parameters,” *J. Vis. Exp.*, no. 47, pp. 1–5, 2011.
- [113] B. Ding, J. Lin, X. Wang, J. Yu, J. Yang, and Y. Cai, “Investigation of silica nanoparticle distribution in nanoporous polystyrene fibers,” *Soft Matter*, vol. 7, no.

18, p. 8376, 2011.

- [114] N. Wang *et al.*, “Multilevel structured polyacrylonitrile/silica nanofibrous membranes for high-performance air filtration,” *Sep. Purif. Technol.*, vol. 126, pp. 44–51, 2014.
- [115] S. Rao, D. Liu, P. Jaiswal, S. Ray, and D. Bhattacharyya, “Electrospun Nanofibre Cores Containing Graphene Oxide for Sandwich Films: Manufacturing and Analysis,” in *Advanced Materials Research*, 2011, vol. 410, pp. 26–30.
- [116] F. Wu, Y. Lu, G. Shao, F. Zeng, and Q. Wu, “Preparation of polyacrylonitrile/graphene oxide by in situ polymerization,” *Polym. Int.*, vol. 61, no. 9, pp. 1394–1399, 2012.
- [117] H. Kim, A. A. Abdala, and C. W. MacOsco, “Graphene/polymer nanocomposites,” *Macromolecules*, vol. 43, no. 16, pp. 6515–6530, 2010.
- [118] T. Pirzada, S. A. Arvidson, C. D. Saquing, S. S. Shah, and S. A. Khan, “Hybrid silica-PVA nanofibers via sol-gel electrospinning,” *Langmuir*, vol. 28, no. 13, pp. 5834–5844, 2012.
- [119] M. Yanilmaz, Y. Lu, J. Zhu, and X. Zhang, “Silica/polyacrylonitrile hybrid nanofiber membrane separators via sol-gel and electrospinning techniques for lithium-ion batteries,” *J. Power Sources*, vol. 313, pp. 205–212, 2016.
- [120] H. R. Jung, D. H. Ju, W. J. Lee, X. Zhang, and R. Kotek, “Electrospun hydrophilic fumed silica/polyacrylonitrile nanofiber-based composite electrolyte membranes,” *Electrochim. Acta*, vol. 54, no. 13, pp. 3630–3637, 2009.
- [121] S. Ahmad, S. Ahmad, and S. A. Agnihotry, “Nanocomposite electrolytes with fumed silica in poly(methyl methacrylate): Thermal, rheological and conductivity studies,” *J. Power Sources*, vol. 140, no. 1, pp. 151–156, 2005.
- [122] J. Liang *et al.*, “Molecular-level dispersion of graphene into poly(vinyl alcohol) and effective reinforcement of their nanocomposites,” *Adv. Funct. Mater.*, vol. 19, no. 14, pp. 2297–2302, 2009.
- [123] R. Rafiq, D. Cai, J. Jin, and M. Song, “Increasing the toughness of nylon 12 by the incorporation of functionalized graphene,” *Carbon N. Y.*, vol. 48, no. 15, pp. 4309–4314, 2010.
- [124] S. Yao, Y. Li, Z. Zhou, and H. Yan, “Graphene oxide-assisted preparation of poly(vinyl alcohol)/carbon nanotube/reduced graphene oxide nanofibers with high carbon content by electrospinning technology,” *RSC Adv.*, vol. 5, no. 111, pp. 91878–91887, 2015.

Vitae

Name : Noman Naseeb

Nationality : Pakistani

Date of Birth : 24-01-1990

Email : nomannaseeb@live.com

Address : House#R-1192 Block 8, Bufferzone, North Nazimabad,
Karachi,75400, Pakistan

Academic Background :

Master of Science in Materials Science and Engineering, 2015-2017

King Fahd University of Petroleum and Minerals, Dhahran, Saudi Arabia

Bachelor of Engineering in Metallurgical, 2009-2012

NED University of Engineering and Technology, Karachi, Pakistan

Publications :

Noman Naseeb, Tahar Laoui, M.A Azeem, Zafarullah Khan, A novel PAN-GO-SiO₂ hybrid membrane for separating oil in water emulsion, In progress.

Noman Naseeb, M.A Azeem, Tahar Laoui, Zafarullah Khan, State of the art in membrane based oil-water separation from emulsified mixtures, In progress.